Statistical wave field theory: Anisotropic wave fields under Neumann's boundary condition

Roland Badeau[a]

[a] *Laboratoire Traitement et Communication de l'Information, Télécom Paris, Institut Polytechnique de Paris, Palaiseau 91120, France*

Abstract

The statistical wave field theory mathematically establishes the statistical laws of the solutions to the wave equation in a bounded domain. It provides the closed-form expressions of the power distribution and the correlations of the wave field jointly over time, frequency, and space, which hold at high frequency and after many reflections, in terms of the geometry and the specific admittance of the boundary surface. This theory was originally developed in the particular case of mixing rooms, which are characterized by a diffuse wave field, based on the theory of dynamical billiards and on Weyl-like asymptotic laws. Then it was extended to the finite family of special polyhedra, where the wave field is anisotropic, based on a simpler geometric approach related to mathematical crystallography. In this paper, we introduce a unified version of the theory dedicated to a class of semi-mixing billiards. In the case of Neumann's boundary condition, we show that the wave field is stationary, but it is generally anisotropic. In particular, the correlation between two spatial positions at a given frequency is different from the well-known cardinal sine formula that characterizes diffuse acoustic fields.

Keywords: Statistical physics, wave equation, Helmholtz equation, quantum billiards

Contents

Email address: `roland.badeau@telecom-paris.fr` (Roland Badeau)

Nomenclature

Acronyms

ACF Auto-covariance function

PDE Partial differential equation

RIR Room impulse response

WSS Wide-sense stationary

Mathematical notations

Be careful: in this paper, we use the Greek letter ψ to denote *any function of any variables* (we do not use the notation f that is usual in mathematics, because here f denotes the frequency). Therefore, the same letter ψ may denote different functions of different variables in different places of the paper, and it is not supposed to have any special physical meaning.

- $\triangleq$: equal by definition to
- $\mathbb{N}$: set of whole numbers

- $\mathbb{R}$, $\mathbb{C}$: sets of real and complex numbers, respectively
- $\imath = \sqrt{-1}$: imaginary unit
- $\boldsymbol{x}$ (bold font), z (regular): vector and scalar, respectively
- $A \backslash B$: relative complement (set difference) of set B in set A
- $A \subseteq B$: A is a subset of B, possibly equal to B
- $\overline{V}$: closure of a subset V of $\mathbb{R}^3$
- $|V|$: Lebesgue measure (volume) of a subset V of $\mathbb{R}^3$
- $\lambda = \frac{1}{|V|}$: mean density of image sources over space
- ∂V: boundary of a subset V of $\mathbb{R}^3$
- $\boldsymbol{n}(\boldsymbol{x})$ where $\boldsymbol{x} \in \partial V$: outward normal to the boundary surface of subset V
- $S(A)$: surface area of a 2-dimensional sub-manifold A of $\mathbb{R}^3$
- $L(C)$: line length of a 1-dimensional sub-manifold C of $\mathbb{R}^3$
- $\|.\|_2$: Euclidean/Hermitian norm of a vector or a function
- $\overline{z}$: complex conjugate of $z \in \mathbb{C}$
- $\boldsymbol{x}^\top$: transpose of vector $\boldsymbol{x}$
- $\boldsymbol{I}$: identity matrix
- $A^\perp$: orthogonal complement of set A
- $\mathcal{S}(0,k)$: sphere centered at the origin and of radius k: $\mathcal{S}(0,k) = \{\boldsymbol{k} \in \mathbb{R}^3; \|\boldsymbol{k}\|_2 = k\}$
- $L^2(V)$ where V is a Borel subset of $\mathbb{R}^3$: Hilbert space of measurable functions f supported in V, such that $\|f\|_2 = \sqrt{\int_V |f(\boldsymbol{x})|^2 d\boldsymbol{x}} < +\infty$
- $\mathcal{S}(\mathbb{R}^n)$: Schwartz space of smooth functions on $\mathbb{R}^n$, whose derivatives of all orders are rapidly decreasing
- $\langle T|\psi\rangle$: value of the tempered distribution T on the test function $\psi \in \mathcal{S}(\mathbb{R}^n)$
- δ: Dirac delta function
- $H(t)$: Heaviside function: $H(t) = 1 \ \forall t > 0$ and $H(t) = 0 \ \forall t < 0$
- $\text{sign}(t)$: sign function: $\text{sign}(t) = 1 \ \forall t > 0$ and $\text{sign}(t) = -1 \ \forall t < 0$
- $\Delta\phi(\boldsymbol{x})$: Laplacian of function $\phi(\boldsymbol{x})$
- $Y_{l,m}(\boldsymbol{u})$ for $l \in \mathbb{N}$, $m \in \{-l, \dots, l\}$, and $\boldsymbol{u} \in \mathcal{S}(0,1)$: real spherical harmonic of degree l and order m;
- 1D direct and inverse Fourier transforms of a function $\psi : \mathbb{R} \to \mathbb{C}$:

$$\begin{aligned} \widehat{\psi}(f) &= \int_{t\in\mathbb{R}} \psi(t) e^{-2\imath\pi f t} dt \\ \text{and} \quad \psi(t) &= \int_{f\in\mathbb{R}} \widehat{\psi}(f) e^{+2\imath\pi f t} df \end{aligned}$$

- 3D direct and inverse Fourier transform of a function $\psi : \mathbb{R}^3 \to \mathbb{C}$:

$$\begin{aligned} \widehat{\psi}(\boldsymbol{k}) &= \int_{\boldsymbol{x}\in\mathbb{R}^3} \psi(\boldsymbol{x}) e^{-2\imath\pi \boldsymbol{k}^\top \boldsymbol{x}} d\boldsymbol{x} \\ \text{and} \quad \psi(\boldsymbol{x}) &= \int_{\boldsymbol{k}\in\mathbb{R}^3} \widehat{\psi}(\boldsymbol{k}) e^{+2\imath\pi \boldsymbol{k}^\top \boldsymbol{x}} d\boldsymbol{k} \end{aligned}$$

- $\mathbb{E}[X]$: expected value of a random variable X
- Covariance of two complex random variables X and Y:

$$\text{cov}[X,Y] = \mathbb{E}[(X - \mathbb{E}[X])\overline{(Y - \mathbb{E}[Y])}]$$

1. Introduction

In room acoustics, under mild physical assumptions, the propagation of waves in a bounded volume V is characterized by the Helmholtz equation under Robin's boundary condition, which is expressed in terms of the specific admittance $\widehat{\beta} \in \mathbb{C}$ with $\mathrm{Re}(\widehat{\beta}) \geq 0$ on the boundary surface ∂V. This boundary value problem admits a discrete set of solutions called *eigenmodes* (Kuttruff, 2014, Chap. 3). When $\widehat{\beta}$ is purely imaginary, which includes the case of rigid surfaces (Neumann's boundary condition, i.e., $\widehat{\beta} = 0$), there is no energy absorption. Then the Laplace operator is self-adjoint, the eigenmodes are real-valued, and they form an orthonormal basis of eigenfunctions of the Laplacian on the Hilbert space of square-integrable functions $L^2(V)$. When on the contrary $\mathrm{Re}(\widehat{\beta}) > 0$, there is energy absorption, the Laplace operator is no longer self-adjoint, its eigenfunctions and generalized eigenfunctions are complex-valued, and it was recently proved that they form an *Abel basis with brackets* of $L^2(V)$ (Badeau, 2025a).

However, in most practical cases, calculating the eigenmodes, given the room geometry and the values of the specific admittance on the boundary, can only be performed numerically and requires extensive computational power. Nevertheless, at high frequency, it is well known that wave propagation can be approximated in the classical limit by considering the trajectory of rays that undergo successive specular reflections on the domain's boundary, similarly to optical rays (Kuttruff, 2014, Chap. 4). The ray trajectory can then be interpreted as a dynamical billiard that, depending on the boundary geometry, may follow different statistical properties (Tabachnikov, 1995). For instance, a classical billiard is *ergodic* when over time t, the position $\boldsymbol{x}(t) \in V$ and the unit direction vector $\boldsymbol{v}(t) \in \mathcal{S}(0,1)$ of almost every ray trajectory are jointly uniformly distributed in the *phase space* $V \times \mathcal{S}(0,1)$, where the *configuration space* (or *position space*) V is the bounded volume of the billiard, and the *momentum space* $\mathcal{S}(0,1)$ is the unit sphere. In other respects, *mixing* billiards, in addition to being ergodic, are such that two different rays that are arbitrarily close in the phase space at $t = 0$ diverge completely after an asymptotically long elapsed time. Under this assumption and when there is no energy absorption at the boundary, the wave field is *diffuse* (Polack, 1992), which means that its statistics are invariant over space under any translation (it is *stationary*), and any rotation (it is *isotropic*). When on the contrary there is energy absorption at the room boundary, then the sound power decreases exponentially over time, at a rate that is uniform in the room and depends on the frequency. The *reverberation time*, often denoted T_{60}, is then defined as the time it takes for the sound pressure level to reduce by 60 dB. In the room acoustics literature, various expressions of the reverberation time in ergodic rooms have been obtained, based on the statistics of the reflections and the mean free path (Joyce, 1978; Polack, 1992; Kuttruff, 2014; Polack, 2025).

In quantum physics, the mathematical framework of *quantum billiards* (Grebenkov and Nguyen, 2013, Sec. 7.7.4) is the same as that in room acoustics, because the solutions of the Schrödinger equation are also characterized by the eigenfunctions of the Laplace operator under Robin's boundary condition. The main difference is that the specific admittance is restricted to purely imaginary values, so the Laplacian is always real, self-adjoint, and its eigenfunctions and eigenvalues are real-valued. In several dimensions of space, it is well known that the density of discrete eigenmodes increases with the frequency, in a way that has been investigated mathematically for the first time by Weyl (1911). Since then, a rich literature has been devoted to the study of asymptotic expansions of the modal density as a function of frequency f when $f \to +\infty$, in various space dimensions and various boundary conditions (Arendt *et al.*, 2009). The case of a three-dimensional (3D) space, which is of special interest to us, was addressed by the physicists Balian and Bloch (1970). Their approach was based on the *semiclassical* approximation of quantum physics (Sieber *et al.*, 1995; Brack and Bhaduri, 1997), which also approximates wave propagation by considering the trajectory of rays undergoing specular reflections, as in classical billiards. However, the mathematical treatment of these reflections explicitly depends on Robin's boundary condition, through the *multiple reflection expansion* of the Green's function, used by Balian and Bloch (1970) and Sieber *et al.* (1995). In addition, such rays can pass through the boundary and re-enter the billiard, as illustrated in Balian and Bloch (1972, Fig. 12). Consequently, the semiclassical approximation is able to account for the curvature of the boundary, through the *two-reflection term* of the series expansion of the Green's function, which allowed Balian and Bloch (1970) to pursue the asymptotic expansion of the modal density up to the second order. Later, the periodic orbit theory showed that each periodic orbit (also called "closed path" by Balian and Bloch (1972)), of length L in the classical billiard, produces a fluctuation of period c/L in the modal density, which is expressed by the Gutzwiller trace formula (Gutzwiller, 1971).

The literature on quantum billiards is actually very rich. Most theorems were established by considering the Dirichlet boundary condition ($\text{Im}(\widehat{\beta}) \to -\infty$), or the Neumann boundary condition ($\widehat{\beta} = 0$), but their conclusions still hold for any purely imaginary value of $\widehat{\beta}$, because their proofs are based on the self-adjoint operator property. The *quantum ergodicity theorem*, established by Zelditch and Zworski (1996), shows that when a classical billiard is ergodic, then asymptotically at high frequency, almost all the eigenfunctions of the Laplacian tend to be uniformly distributed in the phase space $V \times \mathcal{S}(0,1)$. In the language of statistical signal processing, that means that almost all the eigenfunctions of the Laplacian behave asymptotically like isotropically distributed *wide sense stationary* (WSS) random processes, as initially conjectured (in different terms) by Berry (1977). Moreover, the *quantum weak mixing theorem* (Zelditch, 2006) shows that when a classical billiard is weak mixing, then asymptotically at high frequency, in addition to being uniformly distributed in the phase space, almost all the eigenfunctions of the Laplacian tend to be pairwise decorrelated. When this property holds for all eigenfunctions, the billiard is said *quantum unique ergodic* (QUE). Then the whole wave field, which is made of a superposition of these eigenfunctions, tends to behave like an isotropic WSS process at high frequency, which means that it is diffuse. This result is remarkable, because it suggests that the mixing assumption usually considered in the room acoustics literature is insufficient to guarantee a truly diffuse wave field: the more constraining QUE property is required. Indeed, there exist ergodic, and even mixing, billiards that are not QUE (Hassell and Hillairet, 2010). In such billiards, there may be a sparse subsequence of localized eigenfunctions that are characterized by *scars*, which means that their energy is essentially concentrated around some classical periodic orbits (Lu *et al.*, 2025). Scarred eigenfunctions are thus non-stationary. However, the *eigenstate stacking theorem* (Lu *et al.*, 2025) shows that, at high frequency, all the eigenfunctions that lie in any spectral band *collectively* tend to produce a uniform power distribution in the phase space. This uniform distribution is guaranteed under a condition of minimal bandwidth: the spectral band must be larger than $\frac{c}{L_{\min}}$, where $L_{\min}$ is the fundamental period of the shortest classical periodic orbit. Therefore, the eigenstate stacking theorem confirms that the mixing assumption is sufficient to get a diffuse wave field, provided that the discrete spectrum is smoothed by a filter of minimal bandwidth $\frac{c}{L_{\min}}$. Note that this filtering eliminates the previously-mentioned fluctuations in the modal density, whose periods are smaller than $\frac{c}{L_{\min}}$. This was expected, since the non-stationary quantum scars and the fluctuations in the modal density are both related to classical periodic orbits.

In Badeau (2024), for the first time in room acoustics, a theory of reverberation was introduced, which inherits the power of the semiclassical approximation, while complying with the previously-mentioned theorems on quantum billiards. This *statistical wave field theory* holds at high frequency and after many reflections on the room boundary. In Badeau (2024), we addressed the case of mixing billiards. Indeed, in mixing billiards, the wave field behaves like an isotropic WSS random process when there is no energy absorption at the boundary, i.e., when $\widehat{\beta}$ is purely imaginary, so it is diffuse, provided that the discrete spectrum is sufficiently smoothed, as previously explained. Then we showed in Badeau (2024, Sec. III E 2) that the asymptotic expansion of the smoothed modal density directly provides us with a closed-form expression of the *power spectrum* of the WSS wave field. Indeed, because the eigenmodes are uncorrelated and carry on average the same quantity of power, the power spectrum is proportional to the smoothed modal density. If on the contrary there is energy absorption, i.e., if $\mathrm{Re}(\widehat{\beta}) > 0$, then the wave field is non-stationary, and the theory shows that its statistics are actually related to the analytic continuation of the smoothed modal density to the domain of complex frequencies. This approach permitted us to obtain the accurate closed-form expression of the reverberation time in mixing rooms (Badeau, 2024, Sec. VI F). Then, in Badeau (2025b), the accuracy of the theory predictions was further improved at lower frequencies, by exploiting the second order *curvature term* of the asymptotic expansion calculated by Balian and Bloch (1970).

So, in both Badeau (2024) and Badeau (2025b), we focused on mixing rooms, in which the reverberation time is independent of the receiver's position and orientation. However, it is well known that in certain non-ergodic room geometries, the reverberation time is still independent of the receiver's position, but it does depend on its orientation (Alary, 2021). In this case, it is sometimes referred to as the *directional reverberation time* (Bilbao and Alary, 2024). The characterization (Nolan *et al.*, 2018; Xu *et al.*, 2022), analysis (Berzborn and Vorländer, 2021; Götz *et al.*, 2023) and synthesis (Alary *et al.*, 2019, 2024) of such *anisotropic wave fields* have recently received much attention in the room acoustics community, but curiously, few works have been devoted to the physical modeling of anisotropic reverberation (Meyer-Kahlen and Schlecht, 2024; Drechsler, 2012; Drechsler and Stephenson, 2012).

In room acoustics, the most famous anisotropic room is the *shoebox room*, whose geometric shape is that of a rectangular cuboid. The directional reverberation time in this shoebox room has been investigated in Bilbao and Alary (2024). Then in Badeau (2025c), we have shown the existence of a few other polyhedra whose properties are similar to those of the rectangular cuboid. These so-called *special polyhedra* are neither mixing nor ergodic, but rather *integrable* in the sense of Arnold's theorem (Arnold and Avez, 1989). This means that the Helmholtz equation can be solved in closed-form subject to various boundary conditions (Dirichlet, Neumann, and even Robin in certain cases). Moreover, all the eigenfunctions are trigonometric polynomials. Based on these closed-form solutions, deriving the equations of the statistical wave field theory proved to be much easier than in the mixing case (Badeau, 2025c). This study of the special polyhedra permitted us to take a very important turn in the development of the statistical wave field theory: we have shown that neither the mixing, nor even the ergodic assumptions were actually necessary to get stationary statistics independent of the source position, provided that the discrete spectra of these special polyhedra are sufficiently smoothed in the wave vector space.

The special polyhedra belong to the larger class of *rational polyhedra*, which have only rational dihedral angles, i.e., angles that are rational multiples of π. Such polyhedra are not classically ergodic, unlike irrational polyhedra, which are known to be ergodic. Similarly, in two space dimensions (2D), *rational polygons* are not classically ergodic in the phase space, but Kerckhoff *et al.* (1986) showed that they are ergodic in the configuration space, and that every ray trajectory uniformly spans a finite set of directions in the momentum space. In addition, the quantum ergodicity theorem in configuration space for rational polygons (Marklof and Rudnick, 2012) shows that, when $\widehat{\beta}$ is purely imaginary, then asymptotically at high frequency, almost all the eigenfunctions of the Laplacian tend to be uniformly distributed in the configuration space, but not in the momentum space. Finally, Arana-Herrera *et al.* (2025) have recently shown that not every, but *almost every* rational polygon is not only classically ergodic, but also weak mixing in the configuration space. The rare exceptions include the set of *almost integrable* polygons, which includes the four integrable ones that are related to the special polyhedra. Therefore, we expect the special polyhedra to be quantum ergodic, but not quantum weak mixing, in the configuration space.

Following these results on rational polygons, we introduce in this paper three classes of classical billiards that will be referred to as *semi-ergodic*, *weak semi-mixing*, and *strong semi-mixing*, respectively, as these billiards are ergodic, weak mixing, and strong mixing, respectively, in the configuration space, but not necessarily in the momentum space. The general class of 3D semi-ergodic billiards is actually very large: it is not restricted to 3D ergodic billiards and rational polyhedra. For instance, it includes all prisms whose basis is a 2D ergodic billiard (possibly including curved boundaries). It also includes all (possibly non-convex) polyhedra, whether their dihedral angles are rational or irrational. We will show that these billiards are characterized by a *directional measure* σ defined on the momentum space $\mathcal{S}(0,1)$, which depends on the particular billiard geometry, and whose closed-form expression involves a series expansion over a basis of real spherical harmonics. Then, based on the quantum ergodicity theorem in configuration space for rational polygons (Marklof and Rudnick, 2012), we will assume that asymptotically at high frequency in semi-ergodic billiards, almost all the eigenfunctions of the Laplacian tend to be uniformly distributed in the configuration space. In addition, based on the quantum weak mixing theorem (Zelditch, 2006) that holds in weak mixing billiards, we will also assume that similarly in weak semi-mixing billiards, almost all the eigenfunctions of the Laplacian tend to be pairwise decorrelated in the configuration space. Finally, based on the eigenstate stacking theorem (Lu *et al.*, 2025), we will assume that in semi-mixing billiards, the wave field behaves like a WSS random process, provided that the spectral measure is sufficiently smoothed in the 3D wave vector space. Consequently, the class of semi-mixing billiards corresponds to rooms where, through spectral smoothing and at high frequency, the wave field is WSS but generally anisotropic when there is no energy absorption[1], and where the reverberation time is independent of the receiver's position but may depend on its orientation when there is energy absorption. The closed-form expressions of the resulting statistics of the anisotropic wave field will naturally involve the directional measure σ.

In this paper, we will focus on the particular case of Neumann's boundary condition. Then in our next paper on anisotropic wave fields, we will address the general case of Robin's boundary condition, which will allow us to provide, for the first time, the general closed-form expression of the directional reverberation time in semi-mixing rooms. The reader may notice that, similarly to Badeau (2025c) and contrary to Badeau (2024, 2025b), the mathematical approach that we will develop here is not explicitly related to the asymptotic expansion of the smoothed modal density; yet the relationship with the modal density still implicitly exists in the particular case of mixing billiards.

This paper is structured as follows. In Sec. 2, we summarize a few fundamental notions regarding wave propagation that are needed to develop the statistical wave field theory. In Sec. 3, we define the three classes of semi-ergodic, weak and strong semi-mixing billiards, and we provide the closed-form expression of their directional measure. In Sec. 4, we briefly present the Wigner time-frequency distribution that will be used to characterize the second-order properties of random processes, and we list the three mathematical assumptions on which the statistical wave field theory relies. Then in Sec. 5 we present the *special* theory dedicated to Neumann's boundary condition. The main results are summarized in Sec. 5.4. Finally, in Sec. 6 we summarize the main contributions of this paper, and we present a few perspectives for future work.

2. Fundamentals of waves revisited

This section summarizes a few fundamental notions regarding wave propagation that are needed in the rest of the paper. Most of these notions are well-known and are described for

[1] As mentioned previously, there is no energy absorption when $\widehat{\beta}$ is purely imaginary. Actually, in semi-mixing billiards, it is necessary to also assume that $\mathrm{Im}(\widehat{\beta}) \leq 0$ in order to guarantee that the wave field is WSS. Indeed, contrary to the case of mixing billiards, where smoothing the discrete spectrum was sufficient to enforce stationarity due to the eigenstate stacking theorem, in semi-mixing billiards, spectral smoothing is only performed locally in the wave vector space, as illustrated in (Badeau, 2025c, Fig. 3). If $\mathrm{Im}(\widehat{\beta}) > 0$, depending on the room geometry, this weaker form of spectral smoothing does not prevent the possible localization of a part of the wave field energy in the vicinity of the boundary, as we will show in our next paper on anisotropic wave fields.

instance in Morse and Ingard (1968). These and other notions were already presented in more details in Badeau (2024, Sec. III).

2.1. Main definitions

In a connected open domain $V \subseteq \mathbb{R}^3$, the homogeneous wave equation states that

$$\Delta p(\boldsymbol{x}, t) - \frac{1}{c^2}\frac{\partial^2 p(\boldsymbol{x}, t)}{\partial t^2} = 0, \tag{1}$$

where $p(\boldsymbol{x}, t)$ is the wave amplitude at position $\boldsymbol{x} \in V$ and time $t \in \mathbb{R}$, Δ is the Laplacian, and c is the propagation speed of the wave. Applying the 1D Fourier transform w.r.t. time to Eq. (1) yields the Helmholtz equation:

$$\Delta \phi(\boldsymbol{x}) + 4\pi^2 k^2 \phi(\boldsymbol{x}) = 0, \tag{2}$$

where the scalar $k = \frac{f}{c}$ is the *wave number* and f denotes the frequency. We note that any solution ϕ to Eq. (2) is an eigenfunction of the Laplace operator, of eigenvalue $-4\pi^2 k^2$.

Given a punctual source position $\boldsymbol{x}_0 \in V$ and a space position $\boldsymbol{x} \in V$, we define the *source response* p as the unique causal solution to the following inhomogeneous wave equation: $\forall t \in \mathbb{R}$,

$$\Delta p(\boldsymbol{x}, \boldsymbol{x}_0, t) - \frac{1}{c^2}\frac{\partial^2 p(\boldsymbol{x}, \boldsymbol{x}_0, t)}{\partial t^2} = -\delta(\boldsymbol{x} - \boldsymbol{x}_0)\dot{\delta}(t). \tag{3}$$

Note that the right member of Eq. (3) involves the derivative of a Dirac delta function over time, in order to account for the fact that the response of a physical source is always zero at the zero frequency (Morse and Ingard, 1968, Chap. 7). Replacing the derivative $\dot{\delta}(t)$ with $\delta(t)$ in Eq. (3) would lead to the usual definition of the *room impulse response* (RIR) $h(\boldsymbol{x}, \boldsymbol{x}_0, t)$ in room acoustics, which is the causal Green's function of the wave equation [Eq. (1)]. Therefore the RIR h is the unique causal primitive of the source response p defined in Eq. (3).

In the free field (i.e., when $V = \mathbb{R}^3$), the source response p is expressed as

$$p(\boldsymbol{x}, \boldsymbol{x}_0, t) = \frac{\dot{\delta}\left(t - \frac{\|\boldsymbol{x} - \boldsymbol{x}_0\|_2}{c}\right)}{4\pi \|\boldsymbol{x} - \boldsymbol{x}_0\|_2}. \tag{4}$$

2.2. Green's function

Given a punctual source position $\boldsymbol{x}_0 \in V$ and a space position $\boldsymbol{x} \in V$, a Green's function G of the Helmholtz equation is a particular solution to the following inhomogeneous Helmholtz equation:

$$\Delta G(\boldsymbol{x}, \boldsymbol{x}_0, k) + 4\pi^2 k^2 G(\boldsymbol{x}, \boldsymbol{x}_0, k) = -\delta(\boldsymbol{x} - \boldsymbol{x}_0). \tag{5}$$

The inverse 1D Fourier transform of G w.r.t. frequency $f = ck$,

$$g(\boldsymbol{x}, \boldsymbol{x}_0, t) = \int_{f \in \mathbb{R}} G(\boldsymbol{x}, \boldsymbol{x}_0, \tfrac{f}{c})\, e^{2\imath\pi f t} df, \tag{6}$$

is such that its time derivative $\dot{g}(\boldsymbol{x}, \boldsymbol{x}_0, t)$ is a solution to Eq. (3). However, depending on the choice of a particular solution G to Eq. (5), the function $\dot{g}(\boldsymbol{x}, \boldsymbol{x}_0, t)$ may not be causal, so in general $\dot{g}(\boldsymbol{x}, \boldsymbol{x}_0, t)$ differs from the causal source response $p(\boldsymbol{x}, \boldsymbol{x}_0, t)$ by a function that is a solution to the homogeneous wave equation [Eq. (1)].

In the free field ($V = \mathbb{R}^3$), any Green's function G solution to Eq. (5) can be written as the translation over space of some Green's function G_0 for a source located at $\boldsymbol{x}_0 = \boldsymbol{0}$:

$$G(\boldsymbol{x}, \boldsymbol{x}_0, k) = G_0(\boldsymbol{x} - \boldsymbol{x}_0, k).$$

In this paper, we will consider the real Green's function

$$G_0(\boldsymbol{z}, k) = \frac{\cos(2\pi k \|\boldsymbol{z}\|_2)}{4\pi \|\boldsymbol{z}\|_2},$$

which is such that function $\dot{g}$ is an odd function of time. In the free field, the relationship between $\dot{g}$ and the source response p in Eq. (4) can be expressed as

$$p(\boldsymbol{x}, \boldsymbol{x}_0, t) = 2H(t)\, \dot{g}(\boldsymbol{x}, \boldsymbol{x}_0, t), \tag{7}$$

where $H(t)$ denotes the Heaviside function, which is such that $H(t) = 1\ \forall t > 0$ and $H(t) = 0$ $\forall t < 0$. The 3D Fourier transform (see Nomenclature) of $G_0(\boldsymbol{z}, k)$ w.r.t. space is

$$\widehat{G}_0(\boldsymbol{k}, k) = \frac{1}{4\pi^2(\|\boldsymbol{k}\|_2^2 - k^2)}, \tag{8}$$

where vector $\boldsymbol{k}$ is called the *wave vector*.

2.3. B-function

In the case of a connected domain $V \subset \mathbb{R}^3$ with boundaries, any Green's function $G(\boldsymbol{x}, \boldsymbol{x}_0, k)$ can generally be analytically continued in a mathematical vicinity $\mathcal{D}$ of V that depends on the domain's geometry and the boundary condition. In some cases, this extension holds in the full space $\mathcal{D} = \mathbb{R}^3$. The B-function on $\mathcal{D} \subseteq \mathbb{R}^3$ is then defined as:

$$B(\boldsymbol{y}, \boldsymbol{x}_0, k) = -\left(\Delta G(\boldsymbol{y}, \boldsymbol{x}_0, k) + 4\pi^2 k^2 G(\boldsymbol{y}, \boldsymbol{x}_0, k)\right). \tag{9}$$

By definition of the Green's function G in Eq. (5), the restriction of the B-function to V is $\delta(\boldsymbol{y} - \boldsymbol{x}_0)$. Reciprocally, when $\mathcal{D} = \mathbb{R}^3$, a particular Green's function G is obtained as:

$$G(\boldsymbol{x}, \boldsymbol{x}_0, k) = \int_{\boldsymbol{y} \in \mathbb{R}^3} G_0(\boldsymbol{x} - \boldsymbol{y}, k)\, B(\boldsymbol{y}, \boldsymbol{x}_0, k) d\boldsymbol{y}, \tag{10}$$

where G_0 is a free-field Green's function. Equation (10) permits us to interpret the B-function as a spatial distribution of image sources in the free field, which collectively generate inside V the same response as that of the single original source within the bounded domain V. In this paper, we focus on Neumann's boundary condition, in which case the B-function is real-valued and does not depend on k, so it will be simply denoted $B(\boldsymbol{y}, \boldsymbol{x}_0)$.

2.4. Neumann's boundary condition

Let us consider a connected domain $V \subset \mathbb{R}^3$, whose boundary ∂V is a Lipschitz continuous 2D manifold (i.e., ∂V is locally the graph of a Lipschitz function). Then Neumann's boundary condition of the Helmholtz equation [Eq. (2)] states that

$$\forall \boldsymbol{x} \in \partial V,\ \frac{\partial \phi(\boldsymbol{x})}{\partial \boldsymbol{n}(\boldsymbol{x})} = 0, \tag{11}$$

where ∂V denotes the boundary surface of V, and $\frac{\partial}{\partial \boldsymbol{n}(\boldsymbol{x})}$ denotes partial differentiation in the direction of the outward normal $\boldsymbol{n}(\boldsymbol{x})$ to this surface at $\boldsymbol{x}$. When the domain V is bounded, the Laplace operator is self-adjoint, and the set of its eigenfunctions, which are the solutions to the Helmholtz equation [Eq. (2)] under the boundary condition in Eq. (11), is discrete and forms an orthonormal basis of the Hilbert space $L^2(V)$. In room acoustics, Eq. (11) models the reflection of sound waves by *hard* (or *rigid*) surfaces, which reflect the wave without absorbing any energy (Kuttruff, 2014, Chap. 3).

3. Semi-ergodic billiards

In this section, the three classes of semi-ergodic billiards mentioned in Sec. 1 are characterized mathematically. In the definitions that follow, $(\boldsymbol{x}(t),\, \boldsymbol{v}(t)) \in V \times \mathcal{S}(0,1)$ denotes the value in the phase space, at time $t \geq 0$, of the ray trajectory that starts at initial position $\boldsymbol{x}(0) = \boldsymbol{x} \in V$ and initial direction $\boldsymbol{v}(0) = \boldsymbol{v} \in \mathcal{S}(0,1)$. In addition, $\sigma(.|\boldsymbol{v})$ denotes a probability measure over $\mathcal{S}(0,1)$, which will be referred to as the *directional measure*.

Definition 1 (Semi-ergodic billiards)**.** *A classical billiard is* semi-ergodic *if and only if, for almost every ray trajectory and for any continuous function ψ defined on the phase space $V \times \mathcal{S}(0,1)$,*

$$\lim_{T\to+\infty} \tfrac{1}{T} \int_0^T \psi(\boldsymbol{x}(t), \boldsymbol{v}(t))\, dt = \int_{\boldsymbol{u}\in\mathcal{S}(0,1)} \int_{\boldsymbol{y}\in V} \psi(\boldsymbol{y}, \boldsymbol{u})\, \tfrac{d\boldsymbol{y}}{|V|}\, d\sigma(\boldsymbol{u}|\boldsymbol{v}). \tag{12}$$

Definition 2 (Weak semi-mixing billiards)**.** *A classical billiard is* weak semi-mixing *if and only if, for any continuous function ψ and measurable function ϕ defined on the phase space $V \times \mathcal{S}(0,1)$,*

$$\begin{aligned}&\lim_{T\to+\infty} \tfrac{1}{T} \int_0^T \Big| \int_{\boldsymbol{v}\in\mathcal{S}(0,1)} \int_{\boldsymbol{x}\in V} \\ &\Big(\psi(\boldsymbol{x}(t), \boldsymbol{v}(t)) - \int_{\boldsymbol{u}\in\mathcal{S}(0,1)} \int_{\boldsymbol{y}\in V} \psi(\boldsymbol{y}, \boldsymbol{u})\, \tfrac{d\boldsymbol{y}}{|V|} d\sigma(\boldsymbol{u}|\boldsymbol{v})\Big)\, \phi(\boldsymbol{x}, \boldsymbol{v})\, \tfrac{d\boldsymbol{x}}{|V|} \tfrac{dS(\boldsymbol{v})}{4\pi} \Big| dt = 0.\end{aligned} \tag{13}$$

Definition 3 (Strong semi-mixing billiards)**.** *A classical billiard is* strong semi-mixing *(or* semi-mixing*) if and only if, for any continuous function ψ and measurable function ϕ defined on the phase space $V \times \mathcal{S}(0,1)$,*

$$\begin{aligned}&\lim_{t\to+\infty} \int_{\boldsymbol{v}\in\mathcal{S}(0,1)} \int_{\boldsymbol{x}\in V} \psi(\boldsymbol{x}(t), \boldsymbol{v}(t)) \phi(\boldsymbol{x}, \boldsymbol{v})\, \tfrac{d\boldsymbol{x}}{|V|} \tfrac{dS(\boldsymbol{v})}{4\pi} \\ =\ &\int_{\boldsymbol{v}\in\mathcal{S}(0,1)} \Big(\int_{\boldsymbol{u}\in\mathcal{S}(0,1)} \int_{\boldsymbol{y}\in V} \psi(\boldsymbol{y}, \boldsymbol{u})\, \tfrac{d\boldsymbol{y}}{|V|} d\sigma(\boldsymbol{u}|\boldsymbol{v})\Big) \int_{\boldsymbol{x}\in V} \phi(\boldsymbol{x}, \boldsymbol{v})\, \tfrac{d\boldsymbol{x}}{|V|} \tfrac{dS(\boldsymbol{v})}{4\pi}.\end{aligned} \tag{14}$$

Note that all strong semi-mixing billiards are weak semi-mixing, and all weak semi-mixing billiards are semi-ergodic. When the directional measure is isotropic (i.e., $d\sigma(\boldsymbol{u}|\boldsymbol{v}) = \frac{1}{4\pi}\, dS(\boldsymbol{u})\ \forall \boldsymbol{v} \in \mathcal{S}(0,1)$), we retrieve the usual definitions of ergodic, weak mixing, and strong mixing billiards, respectively. Let us now investigate the classical properties of semi-ergodic billiards introduced in Definition 1. Equation (12) shows that the configuration space V and the momentum space $\mathcal{S}(0,1)$ are explored independently by almost every ray trajectory. Moreover, V is explored uniformly over time, and $\mathcal{S}(0,1)$ is explored according to the probability measure σ. More precisely, if $\boldsymbol{v} = \boldsymbol{v}(0)$ is the initial direction of the ray trajectory, then over time t the ray explores the directions $\boldsymbol{u} \in \mathcal{S}(0,1)$ according to the probability measure $d\sigma(\boldsymbol{u}|\boldsymbol{v})$. As previously mentioned, ergodic billiards correspond to the particular case $d\sigma(\boldsymbol{u}|\boldsymbol{v}) = \frac{1}{4\pi} dS(\boldsymbol{u})\ \forall \boldsymbol{v} \in \mathcal{S}(0,1)$ (see Remark 2), whereas special polyhedra are characterized by a discrete directional measure $d\sigma(\boldsymbol{u}|\boldsymbol{v})$ on $\mathcal{S}(0,1)$, whose support contains $\boldsymbol{v}$ (the example of the 2D rectangular billiard is illustrated in Fig. 1; see Remark 3). The aim of the following developments is to express the directional measure σ in closed form, based on Eq. (12).

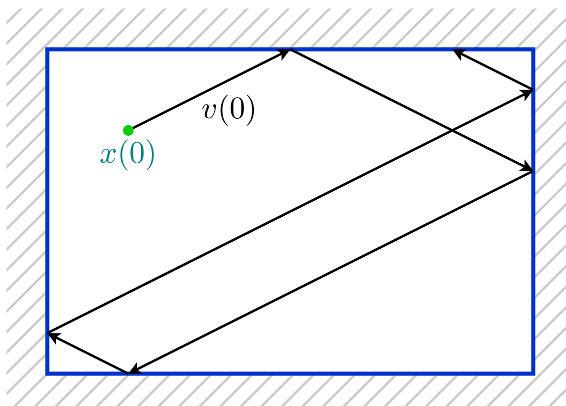

Figure 1: Example of ray trajectory in the classical rectangular billiard. The discrete directional measure σ assigns the same weight to the four directions taken by the ray trajectory, including $\boldsymbol{v}(0)$. The trajectory is interrupted after six reflections to avoid overloading the figure, but after that it will explore space uniformly over time.

First, if we focus on the direction set $\mathcal{S}(0,1)$ independently of the physical space V, Eq. (12) implies that for almost every ray trajectory $(\boldsymbol{x}(t), \boldsymbol{v}(t)) \in V \times \mathcal{S}(0,1)$, for any continuous function ψ defined on $\mathcal{S}(0,1)$,

$$\lim_{T\to+\infty} \frac{1}{T} \int_0^T \psi(\boldsymbol{v}(t))\, dt = \int_{\boldsymbol{u}\in\mathcal{S}(0,1)} \psi(\boldsymbol{u})\, d\sigma(\boldsymbol{u}|\boldsymbol{v}), \tag{15}$$

where $\boldsymbol{v} = \boldsymbol{v}(0)$ is the initial direction of the ray trajectory. Let us now focus on the particular case of special polyhedra. In Badeau (2025c, Sec. II), we introduced these polyhedra, which include the rectangular cuboid, as a particular class of billiards that are *integrable* in the sense of Arnold's theorem (Arnold and Avez, 1989). More precisely, in Badeau (2025c, Sec.

II), these billiards were characterized as the finite set of polyhedra V that strictly tessellate space, which means that $\mathbb{R}^3 = \cup_{j \in \mathbb{Z}} V_j$, where all V_j are isometric to V, and are obtained by reflecting V across its boundary faces. Furthermore, the planes that contain the boundary faces of each V_j have empty intersection with the interior of V_k, for all j and k. To get a clear view of this geometric property of the special polyhedra, which is related to mathematical crystallography, we refer the reader to Badeau (2025c, Fig. 2). In two dimensions, the particular case of the hemiequilateral triangle is illustrated in Fig. 2, where the original polygon V is painted green, and its reflections V_j are left empty. Then, considering the strict tessellation of $\mathbb{R}^3$ by the infinitely many images of V through successive reflections, it is clear that any ray trajectory that undergoes successive specular reflections over the billiard's boundary can equivalently be represented by considering a straight half-line crossing $\mathbb{R}^3$ (red arrow in Fig 2). Therefore, the average of function ψ that is expressed in the left member of Eq. (15) is equivalently obtained as the average of the various images of ψ under the finite point group of isometries generated by the reflections through all faces of V, which is expressed by the integral w.r.t. a discrete directional measure σ in the right member of Eq. (15), whose support contains the initial direction $\boldsymbol{v} = \boldsymbol{v}(0)$ (small black arrow in Fig. 2). This average, as a function of $\boldsymbol{v}$, is thus invariant under this finite point group of isometries.

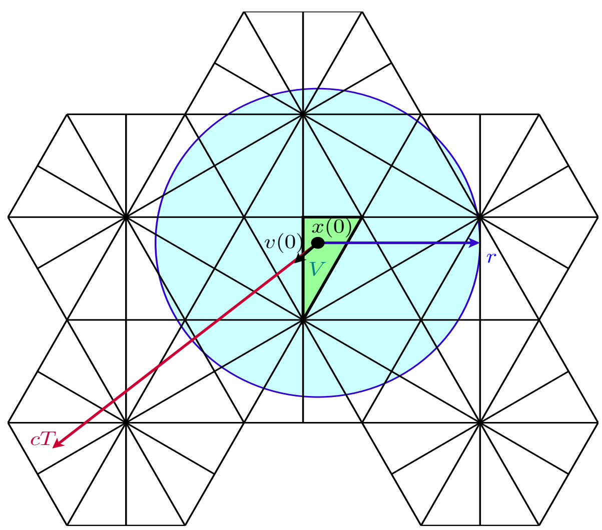

Figure 2: Strict space tessellation by the hemiequilateral triangle. The original polygon V is painted green, and its reflections V_j are left empty. The original position $\boldsymbol{x}(0)$ [resp. direction $\boldsymbol{v}(0)$] of the ray trajectory is represented by the small black disk (resp. small black arrow). The meanings of the blue disk and blue arrow, as well as the red arrow, are explained in Remark 6.

Actually, the same process occurs in all ergodic billiards: the average of function ψ that is expressed in the left member of Eq. (15) is equivalently obtained as the average of the various images of ψ under *all* isometries, which is characterized by the uniform measure $d\sigma(\boldsymbol{u}|\boldsymbol{v}) = \frac{1}{4\pi} dS(\boldsymbol{u})\ \forall \boldsymbol{v} \in \mathcal{S}(0,1)$ in the right member of this equation (see Remark 2). This average is thus *isotropic*, i.e., completely independent of the initial direction $\boldsymbol{v} = \boldsymbol{v}(0)$.

Since the special polyhedra on the first hand, and the ergodic billiards on the other hand, form two extreme cases in the class of semi-ergodic billiards (the former produce the most anisotropic wave fields, while the latter result in complete isotropy), we will admit that in the general case, the average of function ψ in the left member of Eq. (15) can still be equivalently obtained by averaging iteratively reflected versions of ψ, making this average, as a function of $\boldsymbol{v}$, invariant under the reflections through all 2D subspaces tangent to ∂V.

In Appendix Appendix A, the directional measure σ is characterized as follows. For all $l \in \mathbb{N}$, let $\boldsymbol{Y}_l$ denote the $(2l+1)$-dimensional column vector of coefficients $Y_{l,m}$, where $\forall m \in \{-l, \dots, l\}$, $Y_{l,m}$ denotes the real spherical harmonic of degree l and order m (Courant and Hilbert, 2004)[2]. Then $\forall l \in \mathbb{N}$, let $\boldsymbol{A}_l$ be the $(2l+1) \times (2l+1)$ real symmetric positive semidefinite matrix

$$\boldsymbol{A}_l = \lambda \int_{\partial V} \Big(\boldsymbol{I} - \Big(\int_{\boldsymbol{u} \in \mathcal{S}(0,1)} \boldsymbol{Y}_l(\boldsymbol{u}) \boldsymbol{Y}_l \left(\boldsymbol{u} - 2(\boldsymbol{n}(\boldsymbol{s})^\top \boldsymbol{u}) \boldsymbol{n}(\boldsymbol{s})\right)^\top dS(\boldsymbol{u})\Big)\Big) dS(\boldsymbol{s}), \tag{16}$$

where $\boldsymbol{I}$ denotes the identity matrix. Then $\forall \boldsymbol{v} \in \mathcal{S}(0,1)$, the directional measure $\sigma(S|\boldsymbol{v})$ of any measurable subset S of the unit sphere $\mathcal{S}(0,1)$ is expressed as

$$\sigma(S|\boldsymbol{v}) = \lim_{L \to +\infty} \int_{\boldsymbol{u} \in S} \sigma_L(\boldsymbol{u}, \boldsymbol{v}) dS(\boldsymbol{u}), \tag{17}$$

where $\forall L \in \mathbb{N}$,

$$\sigma_L(\boldsymbol{u}, \boldsymbol{v}) = \sum_{l=0}^{L} \boldsymbol{Y}_l(\boldsymbol{v})^\top \mathrm{Proj}_{\mathrm{Ker}(\boldsymbol{A}_l)} \boldsymbol{Y}_l(\boldsymbol{u}). \tag{18}$$

Since the series expansion over spherical harmonics in Eq. (18) is truncated to degree L, $\boldsymbol{u} \mapsto \sigma_L(\boldsymbol{u}, \boldsymbol{v})$ can be interpreted as a smooth density function over $\mathcal{S}(0,1)$, which can be equivalently obtained by smoothing the (possibly discrete) directional measure σ defined in Eq. (17), over the set of unit direction vectors $\boldsymbol{u} \in \mathcal{S}(0,1)$.

It is important to note that the density function $\sigma_L(\boldsymbol{u}, \boldsymbol{v})$ in Eq. (18) explicitly depends on the room geometry through the projections $\mathrm{Proj}_{\mathrm{Ker}(\boldsymbol{A}_l)}$, since the definition of matrix $\boldsymbol{A}_l$ in Eq. (16) involves an integral over the boundary surface ∂V and its outward normal vectors. Consequently, the directional measure σ in Eq. (17) also depends on the room geometry.

Remark 1 (Properties of function σ_L and measure σ)**.** *Let us first investigate a few properties of the bivariate function $\sigma_L(\boldsymbol{u}, \boldsymbol{v})$ introduced in Eq. (18). First, $\sigma_L(\boldsymbol{u}, \boldsymbol{v})$ is a real-valued analytic function of $\boldsymbol{u}$ and $\boldsymbol{v}$, since the spherical harmonics are analytic functions. Moreover, it is symmetric (i.e., $\sigma_L(\boldsymbol{v}, \boldsymbol{u}) = \sigma_L(\boldsymbol{u}, \boldsymbol{v})$), and such that $\sigma_L(\boldsymbol{u}, \boldsymbol{u}) \geq 0$. In addition, the parity of the spherical harmonics implies that $\sigma_L(-\boldsymbol{u}, -\boldsymbol{v}) = \sigma_L(\boldsymbol{u}, \boldsymbol{v})$. When $L \to +\infty$, σ introduced in Eq. (17) is indeed a measure, i.e., $\sigma(S|\boldsymbol{v}) \geq 0$ $\forall S \subset \mathcal{S}(0,1)$[3]. Finally, note that for $l = 0$, the 1×1 matrix $\boldsymbol{A}_0$ is zero, therefore $\mathrm{Proj}_{\mathrm{Ker}(\boldsymbol{A}_0)} = 1$, whereas $\forall l > 0$, $\int_{\boldsymbol{u} \in \mathcal{S}(0,1)} \boldsymbol{Y}_l(\boldsymbol{u})\, dS(\boldsymbol{u}) = 0$. This implies that $\forall \boldsymbol{v} \in \mathcal{S}(0,1)$, $\sigma\left(\mathcal{S}(0,1)|\boldsymbol{v}\right) = \int_{\boldsymbol{u} \in \mathcal{S}(0,1)} Y_{0,0}^2\, dS(\boldsymbol{u}) = 1$, and in the same*

[2] Note that all formulas in Sec. 3 are independent of the choice of a particular spherical coordinate system.
[3] This is a consequence of Eqs. (A.6) and (A.15) in Appendix Appendix A.

way, $\forall L \in \mathbb{N}$, $\int_{\boldsymbol{u}\in\mathcal{S}(0,1)} \sigma_L(\boldsymbol{u},\boldsymbol{v})\, dS(\boldsymbol{u}) = 1$. *Therefore, the directional measure* σ *and the smooth density function* σ_L *sum to one on* $\mathcal{S}(0,1)$*, like a probability measure and a probability density function, respectively.*

Remark 2 (Ergodic billiards)**.** *In the particular case of ergodic billiards, matrix* $\boldsymbol{A}_l$ *is non-singular* $\forall l > 0$*, therefore* $\mathrm{Ker}(\boldsymbol{A}_l) = \{\boldsymbol{0}\}$*. Then Eqs.* (17) *and* (18) *yield* $\forall \boldsymbol{u},\boldsymbol{v} \in \mathcal{S}(0,1)$,

$$d\sigma(\boldsymbol{u}|\boldsymbol{v}) = Y_{0,0}^2\, dS(\boldsymbol{u}) = \tfrac{1}{4\pi}\, dS(\boldsymbol{u}). \tag{19}$$

Remark 3 (Special polyhedra)**.** *In the case of special polyhedra, Eqs.* (17) *and* (18) *are equivalent to*

$$\sigma(\boldsymbol{u}|\boldsymbol{v}) = \tfrac{1}{|\mathrm{D}_{nh}|} \sum_{\boldsymbol{Q}\in\mathrm{D}_{nh}} \delta_{\mathcal{S}(0,1)}(\boldsymbol{u}, \boldsymbol{Q}\,\boldsymbol{v}),$$

where $\delta_{\mathcal{S}(0,1)}$ *denotes the Dirac distribution on the unit sphere, and* D_{nh} *is the finite dihedral point group of isometries* $\boldsymbol{Q}$ *generated by all the reflections through the polyhedron's faces*[4].

In particular, we note that, depending on the domain's geometry, the directional measure σ introduced in Eq. (17) may or may not admit a continuous density w.r.t. the spherical measure.

The following remark is proved in Appendix Appendix A.

Remark 4 (Parity of function σ_L)**.** *For almost every* $\boldsymbol{s} \in \partial V$*, for any function* ψ *defined on* $\mathcal{S}(0,1)$*, we can write*

$$\int_{\boldsymbol{u}\in\mathcal{S}(0,1)} \psi(\boldsymbol{u})\, \sigma_L(\boldsymbol{u}, \boldsymbol{n}(\boldsymbol{s}))\, dS(\boldsymbol{u}) = \int_{\boldsymbol{u}\in\mathcal{S}(0,1)} \tfrac{\psi(\boldsymbol{u})+\psi(-\boldsymbol{u})}{2}\, \sigma_L(\boldsymbol{u}, \boldsymbol{n}(\boldsymbol{s}))\, dS(\boldsymbol{u}). \tag{20}$$

This property will allow us, everywhere in Appendix Appendix B, to replace any function ψ *that is integrated w.r.t. the measure* $\sigma_L(\boldsymbol{u}, \boldsymbol{n}(\boldsymbol{s}))\, dS(\boldsymbol{u})$ *by the symmetrized function* $\frac{\psi(\boldsymbol{u})+\psi(-\boldsymbol{u})}{2}$*, without modifying the value of the integral.*

Remark 5 (Restriction to spherical harmonics of even degree)**.** *Following Remark 4, everywhere in Sec. 5.1, we will consider* $\boldsymbol{v} = \boldsymbol{n}(\boldsymbol{s})$ *and symmetrized functions* $\frac{\psi(\boldsymbol{u})+\psi(-\boldsymbol{u})}{2}$*, which are even. Consequently, the spherical harmonics* $Y_{l,m}(\boldsymbol{u})$ *of odd degree* l*, which are odd functions of* $\boldsymbol{u}$*, vanish in the last integral of Eq.* (20)*. This property makes it possible to consider only the spherical harmonics of even degree when computing such integrals numerically.*

4. Fundamentals of the statistical wave field theory

4.1. Wigner distribution

In Sec. 5, we will consider a random process $q(\boldsymbol{x}, \boldsymbol{x}_0, t)$ that is equal to the causal source response $p(\boldsymbol{x}, \boldsymbol{x}_0, t)$ introduced in Sec. 2.1 for $t \geq 0$ [see Eq. (32)]. In signal processing, the

[4] In Badeau (2025c), we were able to reduce the average over the dihedral point group D_{nh} to a simpler average over the cyclic crystallographic point group C_n, because the underlying vector $\boldsymbol{v}$ was an outward normal to the boundary surface, which implies additional symmetries, as explained in Remark 4.

standard tool for characterizing the second-order statistics of a random process is the *Wigner distribution* (Cohen, 1989), also known as the Wigner-Ville distribution, which describes how the power of this random process is distributed in the time-frequency plane. Let

$$\Gamma_q(\boldsymbol{x}_1, \boldsymbol{x}_2, \boldsymbol{x}_0, t_1, t_2) = \mathrm{cov}[q(\boldsymbol{x}_1, \boldsymbol{x}_0, t_1), q(\boldsymbol{x}_2, \boldsymbol{x}_0, t_2)], \tag{21}$$

which denotes the *auto-covariance function* (ACF) of the random process $q(\boldsymbol{x}, \boldsymbol{x}_0, t)$. Its *cross-Wigner distribution* W_q is then defined as follows: $\forall \boldsymbol{x}_1, \boldsymbol{x}_2, \boldsymbol{x}_0 \in V$, $\forall f, t \in \mathbb{R}$,

$$W_q(\boldsymbol{x}_1, \boldsymbol{x}_2, \boldsymbol{x}_0, f, t) = \int_{\mathbb{R}} \Gamma_q(\boldsymbol{x}_1, \boldsymbol{x}_2, \boldsymbol{x}_0, t + \tfrac{\tau}{2}, t - \tfrac{\tau}{2})\, e^{-2\imath\pi f \tau} d\tau. \tag{22}$$

The cross-Wigner distribution $W_q(\boldsymbol{x}_1, \boldsymbol{x}_2, \boldsymbol{x}_0, f, t)$ in Eq. (22) can be interpreted as the covariance of the random process q between two positions $\boldsymbol{x}_1$ and $\boldsymbol{x}_2$, at fixed frequency f and time t, when the source is located at $\boldsymbol{x}_0$.

Note that the definition of the cross-Wigner distribution in Eq. (22) can equivalently be written as an integral over frequency instead of an integral over time:

$$W_q(\boldsymbol{x}_1, \boldsymbol{x}_2, \boldsymbol{x}_0, f, t) = \textstyle\int_{\mathbb{R}} \mathrm{cov}[\widehat{q}(\boldsymbol{x}_1, \boldsymbol{x}_0, f + \frac{\xi}{2}), \widehat{q}(\boldsymbol{x}_2, \boldsymbol{x}_0, f - \frac{\xi}{2})]\, e^{+2\imath\pi\xi t} d\xi, \tag{23}$$

where $\widehat{q}(\boldsymbol{x}, \boldsymbol{x}_0, f)$ is the 1D Fourier transform of $q(\boldsymbol{x}, \boldsymbol{x}_0, t)$.

In applications, it may be more convenient to consider the cross-Wigner distribution of the RIR $h(\boldsymbol{x}, \boldsymbol{x}_0, t)$ rather than that of the random process $q(\boldsymbol{x}, \boldsymbol{x}_0, t)$. Since $h(\boldsymbol{x}, \boldsymbol{x}_0, t)$ is the unique causal primitive of $p(\boldsymbol{x}, \boldsymbol{x}_0, t)$ as explained in Sec. 2.1, and since $q(\boldsymbol{x}, \boldsymbol{x}_0, t)$ is equal to $p(\boldsymbol{x}, \boldsymbol{x}_0, t)$ for all $t \geq 0$, we get

$$\forall t \geq 0,\ h(\boldsymbol{x}, \boldsymbol{x}_0, t) = \int_0^t q(\boldsymbol{x}, \boldsymbol{x}_0, \tau) d\tau. \tag{24}$$

From now on, the support of $h(\boldsymbol{x}, \boldsymbol{x}_0, t)$ will be extended to negative times by applying Eq. (24) to all $t \in \mathbb{R}$. Then, since $q(\boldsymbol{x}, \boldsymbol{x}_0, \tau)$ is the time derivative of $h(\boldsymbol{x}, \boldsymbol{x}_0, t)$, we get $\widehat{q}(\boldsymbol{x}, \boldsymbol{x}_0, f) = \imath 2\pi f\, \widehat{h}(\boldsymbol{x}, \boldsymbol{x}_0, f)$, thus Eq. (23) yields

$$W_q(\boldsymbol{x}_1, \boldsymbol{x}_2, \boldsymbol{x}_0, f, t) = 4\pi^2 \textstyle\int_{\mathbb{R}} (f^2 - \frac{\xi^2}{4})\, \mathrm{cov}[\widehat{h}(\boldsymbol{x}_1, \boldsymbol{x}_0, f + \frac{\xi}{2}), \widehat{h}(\boldsymbol{x}_2, \boldsymbol{x}_0, f - \frac{\xi}{2})]\, e^{+2\imath\pi\xi t} d\xi.$$

By applying the definition of the cross-Wigner distribution in Eq. (23) to $h(\boldsymbol{x}, \boldsymbol{x}_0, t)$ instead of $q(\boldsymbol{x}, \boldsymbol{x}_0, t)$, we thus finally get the general relationship between $W_q(\boldsymbol{x}_1, \boldsymbol{x}_2, \boldsymbol{x}_0, f, t)$ and $W_h(\boldsymbol{x}_1, \boldsymbol{x}_2, \boldsymbol{x}_0, f, t)$,

$$W_q(\boldsymbol{x}_1, \boldsymbol{x}_2, \boldsymbol{x}_0, f, t) = \left(4\pi^2 f^2 + \frac{1}{4}\frac{\partial^2}{\partial t^2}\right) W_h(\boldsymbol{x}_1, \boldsymbol{x}_2, \boldsymbol{x}_0, f, t). \tag{25}$$

4.2. Mathematical assumptions

The statistical wave field theory relies on three mathematical assumptions:

- Assumption 1: the source's position is a random variable uniformly distributed in V;
- Assumption 2: the frequency f (or equivalently the wave number k) is large;

- Assumption 3: the mean and covariances of the B-function are stationary (in the particular case of Neumann's boundary condition).

The first assumption turns the source response $p(\boldsymbol{x}, \boldsymbol{x}_0, t)$ introduced in Eq. (3) and the B-function $B(\boldsymbol{y}, \boldsymbol{x}_0)$ introduced in Eq. (9) into random processes. In Badeau (2024) and Badeau (2025b), this assumption was presented as a consequence of the mixing property. Yet, in the case of special polyhedra, which are neither mixing nor ergodic, we showed in Badeau (2025c) that sticking to this assumption just results in smoothing the spectral measure of the stationary B-function in the wave vector space, which is consistent with the second and third assumptions. In other respects, assuming that the B-function is stationary (third assumption) amounts to assuming that the receiver's position is uniformly distributed in the room. Then, due to the acoustic reciprocity principle, this assumption also amounts to assuming that the source's position is uniformly distributed in the room.

The second assumption makes it possible to approximate wave propagation by considering the trajectory of rays, and thus to use the mathematical framework of the dynamical billiard theory, as already explained in Sec. 1. More precisely, we consider the same semiclassical approximation as in Balian and Bloch (1970) and Sieber *et al.* (1995). In Badeau (2024) and Badeau (2025b), this assumption permitted us to apply *spectral smoothing*, i.e., to approximate the discrete modal distribution by a smooth modal density, and to consider asymptotic expansions of various functions of the frequency, including the modal density. In addition, this assumption permits us to locally approximate a possibly curved boundary surface by its tangent plane, as we already did in Badeau (2024).

Last, the third assumption implies that the wave field statistics are independent of the receiver's position. As explained in Sec. 1, this assumption is consistent with the semi-mixing property introduced in Definition 3, provided that the spectral measure is sufficiently smoothed in the wave vector space. Mathematically, in the case of Neumann's boundary condition, we will thus assume that the B-function is a real WSS random process, which means that both its mean $\mu_B = \mathbb{E}[B(\boldsymbol{y}, \boldsymbol{x}_0)]$ and its covariances $\text{cov}[B(\boldsymbol{y}+\boldsymbol{z}, \boldsymbol{x}_0), B(\boldsymbol{y}, \boldsymbol{x}_0)]$ are well-defined and do not depend on $\boldsymbol{y}$. Its stationary first and second order statistics are then characterized by the mean $\mu_B = \lambda \triangleq \frac{1}{|V|}$ (as proved in Badeau (2024, Sec. IV D 1)), the ACF $\Gamma_B(\boldsymbol{z}) \triangleq \text{cov}[B(\boldsymbol{y}+\boldsymbol{z}, \boldsymbol{x}_0), B(\boldsymbol{y}, \boldsymbol{x}_0)]$, and its 3D Fourier transform, the anisotropic *spectral measure* $\widehat{\Gamma}_B(\mathcal{K})$, whose closed-form expression will be established in Appendix Appendix B.3.

5. Special statistical wave field theory

In the case of Neumann's boundary condition, the B-function is WSS, as explained in Sec. 4.2, so the room response $p(\boldsymbol{x}, \boldsymbol{x}_0, t)$ to a punctual source is WSS over both space and time, and it can be decomposed onto the set of plane waves $e^{2\imath\pi \boldsymbol{k}^\top \boldsymbol{x}} \cos(2\pi c \|\boldsymbol{k}\|_2 t)$ for all wave vectors $\boldsymbol{k} \in \mathbb{R}^3$ [Eqs. (32) and (33)]. Then the purpose of the special statistical wave field theory is to calculate the spectral measure $\widehat{\Gamma}_B(\mathcal{K})$ [Eq. (29)], which can be interpreted as the power distribution of the plane waves in this decomposition.

5.1. Asymptotic expansion of the spectral measure

Based on the mathematical developments in Appendix Appendix B, at finite degree L of the series expansion over spherical harmonics, the B-function is a WSS random process of mean $\mu_B = \lambda$ and of power spectrum

$$\widehat{\Gamma}_L(\boldsymbol{k}) = \lambda\Big(1 + \tfrac{\lambda}{4}\int_{\boldsymbol{s}\in\partial V}\Big(\int_{\boldsymbol{u}\in\mathcal{S}(0,1)}\delta\left(\boldsymbol{u}^\top\boldsymbol{k}\right)\,\sigma_L(\boldsymbol{u},\boldsymbol{n}(\boldsymbol{s}))\,dS(\boldsymbol{u})\Big)dS(\boldsymbol{s})\Big), \tag{26}$$

where $\sigma_L(\boldsymbol{u},\boldsymbol{v})$ was defined in Eq. (18). In Appendix Appendix B, it is shown that $\widehat{\Gamma}_L(\boldsymbol{k})$ is an analytic function of $\boldsymbol{k}$ on $\mathbb{R}^3\backslash\{\boldsymbol{0}\}$.

Then the spectral representation theorem (Theorem 8.4.IV in Daley and Vere-Jones (2003, Chap. 8)) shows that the random process $B(\boldsymbol{y},\boldsymbol{x}_0)$ can be represented as[5]:

$$B(\boldsymbol{y},\boldsymbol{x}_0) = \lambda + \int_{\boldsymbol{k}\in\mathbb{R}^3} e^{2\imath\pi\boldsymbol{k}^\top(\boldsymbol{y}-\boldsymbol{x}_0)}d\widehat{B}_L(\boldsymbol{k}), \tag{27}$$

where $\widehat{B}_L$ is a centered complex random measure with uncorrelated increments $d\widehat{B}_L(\boldsymbol{k})$ on $\mathbb{R}^3$, which is Hermitian symmetric w.r.t. $\boldsymbol{k}$, such that for any Borel set $\mathcal{K}\subset\mathbb{R}^3$,

$$\mathbb{E}\left[\left(\widehat{B}_L(\mathcal{K})\right)^2\right] = 0\,\text{and}\,\mathbb{E}\left[\left|\widehat{B}_L(\mathcal{K})\right|^2\right] = \int_{\boldsymbol{k}\in\mathcal{K}}\widehat{\Gamma}_L(\boldsymbol{k})d\boldsymbol{k}. \tag{28}$$

Finally, when $L\to+\infty$, the sequence of analytic functions $\widehat{\Gamma}_L(\boldsymbol{k})$ defined in Eq. (26) converges in the sense of distributions to a spectral measure $\widehat{\Gamma}_B$ on $\mathbb{R}^3$, which is defined as $\forall\mathcal{K}\subset\mathbb{R}^3$,

$$\widehat{\Gamma}_B(\mathcal{K}) = \int_{\boldsymbol{k}\in\mathcal{K}}\lambda\Big(1 + \tfrac{\lambda}{4}\int_{\boldsymbol{s}\in\partial V}\Big(\int_{\boldsymbol{u}\in\mathcal{S}(0,1)}\delta\left(\boldsymbol{u}^\top\boldsymbol{k}\right)\,d\sigma(\boldsymbol{u}|\boldsymbol{n}(\boldsymbol{s}))\Big)dS(\boldsymbol{s})\Big)d\boldsymbol{k}, \tag{29}$$

where the directional measure σ was expressed in Eq. (17). As explained in Remarks 2 and 3, Eq. (29) encompasses both particular cases of mixing billiards and of special polyhedra since it generalizes the closed-form expressions of the spectral measure in Badeau (2025c, Secs. V B and VII).

5.2. Green's function

Substituting Eqs. (8) and (27) into Eq. (10) leads to the following spectral representation of the Green's function:

$$G(\boldsymbol{x},\boldsymbol{x}_0,k) = \mu_G(k) + \int_{\boldsymbol{k}\in\mathbb{R}^3}\frac{e^{2\imath\pi\boldsymbol{k}^\top(\boldsymbol{x}-\boldsymbol{x}_0)}}{4\pi^2(\|\boldsymbol{k}\|_2^2 - k^2)}d\widehat{B}_L(\boldsymbol{k}), \tag{30}$$

where

$$\mu_G(k) = \lambda\,\widehat{G}_0(\boldsymbol{0},k) = -\frac{\lambda}{4\pi^2k^2}. \tag{31}$$

[5] Note that the source position $\boldsymbol{x}_0$ is subtracted from $\boldsymbol{y}$ in Eq. (27). This adjustment makes this equation independent of the choice of the origin of space, and respects the acoustic reciprocity principle: Eq. (27) would be unchanged by switching $\boldsymbol{y}$ and $\boldsymbol{x}_0$.

5.3. Source response

In Appendix Appendix C, based on the spectral representation of the Green's function in Eq. (30), the causal source response p introduced in Eq. (3) is expressed as

$$p(\boldsymbol{x}, \boldsymbol{x}_0, t) = H(t)\, q(\boldsymbol{x}, \boldsymbol{x}_0, t), \tag{32}$$

where the random process q is defined by the following spectral representation:

$$q(\boldsymbol{x}, \boldsymbol{x}_0, t) = c^2 \left(\lambda + \int_{\boldsymbol{k}\in\mathbb{R}^3} \cos(2\pi c\|\boldsymbol{k}\|_2 t) e^{2\imath\pi \boldsymbol{k}^\top(\boldsymbol{x}-\boldsymbol{x}_0)} d\widehat{B}_L(\boldsymbol{k})\right). \tag{33}$$

Based on Eq. (33), the ACF Γ_q of the random process q defined in Eq. (21) is a tempered distribution, so that $\forall \psi(f) \in \mathcal{S}(\mathbb{R})$ such that $\psi(0) = 0$ at $f = 0$[6],

$$\begin{aligned} & \left\langle \Gamma_q(\boldsymbol{x}_1, \boldsymbol{x}_2, \boldsymbol{x}_0, t + \tfrac{\tau}{2}, t - \tfrac{\tau}{2}) \middle| \widehat{\psi}(\tau) \right\rangle \\ = \; & \tfrac{c^4}{4} \int_{\boldsymbol{k}\in\mathbb{R}^3} \cos(2\pi \boldsymbol{k}^\top(\boldsymbol{x}_1 - \boldsymbol{x}_2)) \left(\psi(c\|\boldsymbol{k}\|_2) + \psi(-c\|\boldsymbol{k}\|_2)\right) \widehat{\Gamma}_L(\boldsymbol{k}) d\boldsymbol{k}, \end{aligned} \tag{34}$$

where we have used Eqs. (28) and (B.7), and we have taken into account the parity of the power spectrum $\widehat{\Gamma}_L(\boldsymbol{k})$ that was expressed in Eq. (26).

5.4. Wigner distribution

By substituting Eq. (34) into Eq. (22)[7], we get the asymptotic expression of the cross-Wigner distribution of the random process q defined in Eq. (33), which holds when $|f| \to +\infty$:

$$W_q(\boldsymbol{x}_1, \boldsymbol{x}_2, \boldsymbol{x}_0, f, t) = \tfrac{c^3}{4} \int_{\boldsymbol{k}\in\mathcal{S}(0, \frac{|f|}{c})} \cos(2\pi \boldsymbol{k}^\top(\boldsymbol{x}_1 - \boldsymbol{x}_2)) \widehat{\Gamma}_L(\boldsymbol{k}) dS(\boldsymbol{k}). \tag{35}$$

As expected, the cross-Wigner distribution $W_q(\boldsymbol{x}_1, \boldsymbol{x}_2, \boldsymbol{x}_0, f, t)$ in Eq. (35) is independent of $\boldsymbol{x}_0$ and t, and it is a function of $\boldsymbol{x}_1 - \boldsymbol{x}_2$, which confirms that the random process $q(\boldsymbol{x}, \boldsymbol{x}_0, t)$ is WSS over both time and space (remember that there is no loss at the boundaries with Newmann's boundary condition). Equation (35) generalizes Eq. (89) in Badeau (2024), which was obtained in the particular case of an isotropic wave field.

When $\boldsymbol{x}_1 = \boldsymbol{x}_2 = \boldsymbol{x}$, we finally get the expression of the power distribution jointly over space, frequency and time, which holds when $|f| \to +\infty$:

$$W_q(\boldsymbol{x}, \boldsymbol{x}, \boldsymbol{x}_0, f, t) = \pi\lambda c \left(f^2 + \tfrac{\lambda c S(\partial V)}{8} |f|\right). \tag{36}$$

Equation (36) is derived in Appendix Appendix D. As expected, this power distribution is independent of $\boldsymbol{x}$, $\boldsymbol{x}_0$ and t, and its closed-form expression is the same as Eq. (91) in Badeau

[6] We can assume that $\psi(0) = 0$ without loss of generality, because the theory holds at high frequency, as explained in Sec. 4.2. This assumption permitted us to simplify the expression of the right member in Eq. (34).

[7] To derive Eq. (35), Eq. (34) can be applied to any sequence of Schwartz functions that converges in the sense of distributions to $\psi(\xi) = \delta(\xi - f)$, so that $\widehat{\psi}(\tau) = e^{-\imath 2\pi f \tau}$.

(2024), which was obtained in the particular case of an isotropic wave field. Finally, as already discussed in Sec. 4.1, it may be more convenient in applications to consider the cross-Wigner distribution of the RIR $h(\boldsymbol{x}, \boldsymbol{x}_0, t)$ rather than that of the random process $q(\boldsymbol{x}, \boldsymbol{x}_0, t)$. By substituting Eq. (25) into Eq. (35), we thus get the asymptotic expansion of $W_h(\boldsymbol{x}_1, \boldsymbol{x}_2, \boldsymbol{x}_0, f, t)$, which holds when $|f| \to +\infty$:

$$W_h(\boldsymbol{x}_1, \boldsymbol{x}_2, \boldsymbol{x}_0, f, t) = \tfrac{c^3}{16\pi^2 f^2} \int_{\boldsymbol{k}\in\mathcal{S}(0,\frac{|f|}{c})} \cos(2\pi \boldsymbol{k}^\top(\boldsymbol{x}_1 - \boldsymbol{x}_2))\widehat{\Gamma}_L(\boldsymbol{k}) dS(\boldsymbol{k}). \tag{37}$$

In the same way, by substituting Eq. (25) into Eq. (36), we get

$$W_h(\boldsymbol{x}, \boldsymbol{x}, \boldsymbol{x}_0, f, t) = \tfrac{\lambda c}{4\pi} \left(1 + \tfrac{\lambda c S(\partial V)}{8|f|}\right). \tag{38}$$

6. Conclusion

In this paper, which focuses on Neumann's boundary condition, we extended the statistical wave field theory introduced in Badeau (2024) to a class of semi-mixing billiards that generate anisotropic wave fields. First, we characterized the statistics of the ray trajectories in semi-ergodic billiards in terms of their directional measure σ. Then we established the closed-form expression of σ, based solely on the geometric shape of the billiard. The formula that we obtained involves a series expansion over a basis of real spherical harmonics [Eqs. (17) and (18)], which gives us a practical way of computing the directional measure numerically, and suggests a possible application of the theory to model late reverberation in modern 3D sound systems involving spherical harmonics (Poletti, 2005). In addition, this series expansion offers a concrete method to determine whether the wave field in a given room is isotropic or anisotropic. Indeed, the wave field is isotropic (and the corresponding dynamical billiard is ergodic) if and only if all terms of non-zero degree in this series expansion are zero (see Remark 2). This approach to quantifying the isotropy of the sound field is based on the solid mathematical grounds of the statistical wave field theory, so we expect it to be more reliable than the experimental methods that have been proposed so far.

In addition, we proved that in semi-mixing billiards, the expression of the Wigner distribution of the source response [Eq. (36)], which describes the power distribution of the wave field over space, frequency and time, is actually the same as that in isotropic (i.e., mixing) rooms that we obtained in Badeau (2024). Consequently, the RIR $h(\boldsymbol{x}, \boldsymbol{x}_0, t)$ is a WSS process, whose power spectral density tends to $\frac{\lambda c}{4\pi}$ when $|f| \to +\infty$, which means that at high frequency, the RIR behaves like white noise. However, still in these semi-mixing billiards, the expression of the cross-Wigner distribution of the source response [Eq. (35)], which describes the covariance of the wave field between two positions at fixed frequency and time, is different from that in isotropic rooms that we obtained in Badeau (2024). Consequently, the spectral correlation over space is anisotropic, therefore different from the well-known expression that characterizes diffuse acoustic fields (Cook *et al.*, 1955).

In our next paper on anisotropic wave fields, we will address the general case of Robin's boundary condition. We will show that when there is energy absorption at the boundary, contrary to the mixing case, at fixed frequency in these semi-mixing billiards, the power distribution is no longer an exponential function of time: the temporal profile of the power distribution is rather a linear combination of infinitely many decreasing exponentials. We will thus retrieve a well-known fact in room acoustics: the time decay in non-ergodic rooms is not exponential (Kanev, 2012; Kuttruff, 2014). However, we will show that such wave fields are characterized by a directional reverberation time that is independent of the receiver's position but depends on its orientation, and we will provide its closed-form expression, which improves and generalizes both Eyring's formula of the reverberation time in ergodic rooms (Eyring, 1930), and Bilbao and Alary's formula of the directional reverberation time in the shoebox room (Bilbao and Alary, 2024). This study of directional reverberation will result in the definition a directional absorption coefficient of the surfaces, which will be explicitly related to the specific admittance of Robin's boundary condition.

Finally, there exists various non-ergodic billiards that do not fall into the category that we investigated in this paper. This is, e.g., the case of all convex geometric shapes with a smooth boundary, including spheres and ellipsoids. In these billiards, the wave field is always non-stationary over space, even when the boundary surface is rigid (in which case the wave field is only stationary over time). We believe that the extension of the statistical wave field theory to such geometric shapes, although of secondary importance in room acoustics, represents a challenge worth taking up, in order to further clarify the relationship between the statistics of the wave field and the statistics of the underlying classical billiard.

Acknowledgments

The author would like to thank the anonymous reviewers for their very helpful comments, which greatly contributed to making this article more accessible.

Author Declarations

Conflict of Interest: The author of this paper has no conflict of interest to disclose.

Data Availability

Data sharing is not applicable to this article as no new data were created or analyzed in this study.

Appendix A.

In this appendix, we prove the results on semi-ergodic billiards presented in Sec. 3.

Appendix A.1. Characterization of the directional measure

In order to calculate the outcome of the dynamic reflection process described in Sec. 3, we consider the following partial differential equation (PDE): $\forall r \geq 0$, $\forall \boldsymbol{u} \in \mathcal{S}(0,1)$,

$$\frac{\partial \psi(\boldsymbol{u},r)}{\partial r} = \lambda \int_{\partial V} \left(\psi\left(\boldsymbol{u} - 2\,(\boldsymbol{n}(\boldsymbol{s})^\top \boldsymbol{u})\boldsymbol{n}(\boldsymbol{s}), r\right) - \psi\left(\boldsymbol{u}, r\right)\right)\, dS(\boldsymbol{s}), \tag{A.1}$$

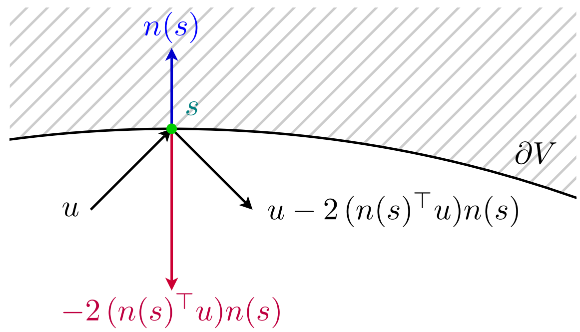

Figure A.3: Specular reflection of the incident vector $\boldsymbol{u}$ at $\boldsymbol{s} \in \partial V$, where $\boldsymbol{n}(\boldsymbol{s})$ is the outward normal to the boundary ∂V at point $\boldsymbol{s}$.

where $\boldsymbol{n}(\boldsymbol{s})$ is the outward normal to the boundary surface ∂V at $\boldsymbol{s}$, and $\boldsymbol{u}-2\left(\boldsymbol{n}(\boldsymbol{s})^\top \boldsymbol{u}\right)\boldsymbol{n}(\boldsymbol{s})$ is the image of the unit vector $\boldsymbol{u}$ by the reflection symmetry through the plane tangent to ∂V at $\boldsymbol{s}$ (its construction is illustrated in Fig. A.3), so that function $\boldsymbol{u} \mapsto \psi\left(\boldsymbol{u}-2\left(\boldsymbol{n}(\boldsymbol{s})^\top \boldsymbol{u}\right)\boldsymbol{n}(\boldsymbol{s}), r\right)$ is the image of function $\boldsymbol{u} \mapsto \psi\left(\boldsymbol{u}, r\right)$ through this reflection symmetry. The initial value at $r=0$ of function $\psi(\boldsymbol{u}, r)$ in Eq. (A.1) is the function $\psi(.)$ introduced in Eq. (15), and the limit of function $\psi(\boldsymbol{u}, r)$ when $r \to \infty$ is the average of the same function $\psi(.)$ through the successive reflections on ∂V, i.e., the left member of Eq. (15).

Remark 6 (Interpretation of Eq. (A.1))**.** *In the particular case of the special polyhedra, function $\psi(\boldsymbol{u}, r)$ for $r \geq 0$ in Eq.* (A.1) *may be equated to the average of function $\psi(.)$ and all its reflections that correspond to the reflected polyhedra V_j that intersect the ball centered at $\boldsymbol{x}(0)$ and of radius r (illustrated in 2D as the blue disk in Fig. 2, where the blue arrow indicates the radius r). Then the limit of function $\psi(\boldsymbol{u}, r)$ when $r \to \infty$ is the average of all the successive reflections of function $\psi(.)$. In the same way, in the general case, making the radius r in Eq.* (A.1) *increase and tend to infinity is equivalent to averaging the images of function $\psi(.)$ through an increasing number of reflections on ∂V. The fact that this average is the same as the left member of Eq.* (15) *(that corresponds to a single ray trajectory, such as that represented by the red arrow in Fig. 2) is a specific property of semi-ergodic billiards.*

Note that integrating Eq. (A.1) over the sphere $\mathcal{S}(0,1)$ yields $\frac{\partial}{\partial r}\int_{\mathcal{S}(0,1)} \psi(\boldsymbol{u}, r) dS(\boldsymbol{u}) = 0$, therefore,

$$\int_{\mathcal{S}(0,1)} \psi(\boldsymbol{u}, \infty) dS(\boldsymbol{u}) = \int_{\mathcal{S}(0,1)} \psi(\boldsymbol{u}, r) dS(\boldsymbol{u}) \;\forall r \geq 0,$$

which means that the integral of function $\psi(\boldsymbol{u}, r)$ is constant over this dynamic reflection process.

Equation (A.1) can be rewritten in the more compact form: $\forall r \geq 0$, $\forall \boldsymbol{u} \in \mathbb{R}^3$,

$$\frac{\partial \psi(\boldsymbol{u}, r)}{\partial r} = -\int_{\boldsymbol{v} \in \mathbb{R}^3} A(\boldsymbol{u}, \boldsymbol{v})\, \psi(\boldsymbol{v}, r) d\boldsymbol{v}, \tag{A.2}$$

where

$$A(\boldsymbol{u},\boldsymbol{v}) = \lambda \int_{\partial V} (\delta\,(\boldsymbol{u}-\boldsymbol{v}) - \delta(\boldsymbol{u}-\boldsymbol{v}+2(\boldsymbol{n}(\boldsymbol{s})^\top \boldsymbol{v})\boldsymbol{n}(\boldsymbol{s})))dS(\boldsymbol{s}). \tag{A.3}$$

Note that Eq. (A.2) holds for a function ψ defined on $\mathbb{R}^3$, even if we are actually interested in the restriction of this function to the subset $\mathcal{S}(0,1)$.

Let us now solve Eq. (A.2). The linear operator A introduced in Eq. (A.3) is clearly self-adjoint, and it is also positive semidefinite. Indeed, for any function $\psi(\boldsymbol{u}) \in L^2(\mathbb{R}^3)$,

$$\begin{aligned}
&\int_{\boldsymbol{u}\in\mathbb{R}^3}\int_{\boldsymbol{v}\in\mathbb{R}^3} \overline{\psi(\boldsymbol{u})} A(\boldsymbol{u},\boldsymbol{v})\psi(\boldsymbol{v})d\boldsymbol{v}d\boldsymbol{u} \\
= \;& \lambda \int_{\partial V}\int_{\boldsymbol{v}\in\mathbb{R}^3} \left(|\psi(\boldsymbol{v})|^2 - \overline{\psi(\boldsymbol{v}-2(\boldsymbol{n}(\boldsymbol{s})^\top \boldsymbol{v})\,\boldsymbol{n}(\boldsymbol{s}))}\psi(\boldsymbol{v})\right) d\boldsymbol{v}\, dS(\boldsymbol{s}).
\end{aligned}$$

However the Cauchy–Schwarz inequality shows that $\forall \boldsymbol{s} \in \partial V$,

$$\left|\int_{\boldsymbol{v}\in\mathbb{R}^3} \overline{\psi(\boldsymbol{v}-2(\boldsymbol{n}(\boldsymbol{s})^\top \boldsymbol{v})\,\boldsymbol{n}(\boldsymbol{s}))}\psi(\boldsymbol{v})d\boldsymbol{v}\right| \leq \int_{\boldsymbol{v}\in\mathbb{R}^3} |\psi(\boldsymbol{v})|^2 d\boldsymbol{v}, \tag{A.4}$$

therefore $\int_{\boldsymbol{u}\in\mathbb{R}^3}\int_{\boldsymbol{v}\in\mathbb{R}^3} \overline{\psi(\boldsymbol{u})} A(\boldsymbol{u},\boldsymbol{v})\psi(\boldsymbol{v})d\boldsymbol{v}d\boldsymbol{u} \geq 0$, which finally proves that A is positive semidefinite. Moreover, the solution to the PDE in Eq. (A.2) can be expressed in the form

$$\psi(.,r) = \exp\left(-Ar\right)\psi(.,0),$$

and since the operator A is self-adjoint and positive semidefinite, when $r \to +\infty$ this solution converges to

$$\psi(.,\infty) = \operatorname{Proj}_{\operatorname{Ker}(A)} \psi(.,0), \tag{A.5}$$

where $\operatorname{Proj}_{\operatorname{Ker}(A)}$ denotes the orthogonal projection onto the kernel of the linear operator A.

Remark 7 (Invariance of Ker(A) under the reflections)**.** *Note that the subspace* Ker(A) *is completely determined by the geometry of ∂V [Eq.* (A.3)*]. Moreover, for any function ψ in this kernel, there is equality in Eq.* (A.4)*. Therefore, $\psi(\boldsymbol{v}) = \psi(\boldsymbol{v}-2(\boldsymbol{n}(\boldsymbol{s})^\top \boldsymbol{v})\,\boldsymbol{n}(\boldsymbol{s}))$ for almost every $\boldsymbol{s} \in \partial V$, which means that the limit $\psi(.,\infty)$ in Eq.* (A.5) *is invariant under the reflections through all 2D subspaces tangent to ∂V, as mentioned in Sec. 3. In particular, any isotropic function, which is of the form $\boldsymbol{v} \mapsto \phi(\|\boldsymbol{v}\|_2)$, belongs to* Ker($A$).

In other respects, if the initial function is such that $\psi(\boldsymbol{u},0) \geq 0\ \forall \boldsymbol{u} \in \mathcal{S}(0,1)$, then we can show by induction that $\forall r \geq 0$, $\psi(\boldsymbol{u},r)\,e^{\lambda S(\partial V)r} \geq \psi(\boldsymbol{u},0) \geq 0$. Indeed, the assertion holds at $r=0$ by assumption, and if it holds up to radius $r>0$, then Eq. (A.1) yields

$$\frac{\partial\left(\psi(\boldsymbol{u},r)\,e^{\lambda S(\partial V)r}\right)}{\partial r} \geq \lambda \int_{\partial V} (0-\psi\,(\boldsymbol{u},r))\,dS(\boldsymbol{s})\,e^{\lambda S(\partial V)r} + \psi(\boldsymbol{u},r)\,\lambda S(\partial V)\,e^{\lambda S(\partial V)r} = 0,$$

so function $\psi(\boldsymbol{u},r)\,e^{\lambda S(\partial V)r}$ is non-decreasing at r, therefore the assertion continues to hold for radii greater than r. We have thus proved that $\forall r \geq 0$, $\psi(\boldsymbol{u},r) \geq \psi(\boldsymbol{u},0)\,e^{-\lambda S(\partial V)r} \geq 0$. When $r \to +\infty$, we get $\psi(\boldsymbol{u},\infty) \geq 0\ \forall \boldsymbol{u} \in \mathcal{S}(0,1)$. We can conclude that the PDE in Eq. (A.2) preserves the non-negativity of the input function,

$$\psi(\boldsymbol{u},0) \geq 0\ \forall \boldsymbol{u} \in \mathcal{S}(0,1) \Rightarrow \psi(\boldsymbol{v},\infty) \geq 0\ \forall \boldsymbol{v} \in \mathcal{S}(0,1). \tag{A.6}$$

Appendix A.2. Series expansion over a basis of spherical harmonics

Finally, we can push further this analysis of the dynamic reflection process by noting that the orthogonal projection in Eq. (A.5) can actually be expressed in closed form. Indeed, the linear operator A defined in Eq. (A.3) is block-diagonalizable in a basis of real spherical harmonics, which is a direct consequence of Eq. (A.12), and which provides a practical way of computing $\mathrm{Proj}_{\mathrm{Ker}(A)}$. To show that, let us first decompose function $\psi(\boldsymbol{u}, r)$ introduced in Eq. (A.1) over a basis of real spherical harmonics: $\forall r \geq 0$, $\forall \boldsymbol{u} \in \mathcal{S}(0,1)$,

$$\psi(\boldsymbol{u}, r) = \sum_{l\in\mathbb{N}} \sum_{m=-l}^{l} \psi_{l,m}(r)\, Y_{l,m}\left(\boldsymbol{u}\right), \tag{A.7}$$

and reciprocally,

$$\psi_{l,m}(r) = \int_{\boldsymbol{u}\in\mathcal{S}(0,1)} Y_{l,m}(\boldsymbol{u})\, \psi(\boldsymbol{u}, r) dS(\boldsymbol{u}), \tag{A.8}$$

where $Y_{l,m}(\boldsymbol{u})$ denotes the real spherical harmonic of degree l and order m (Courant and Hilbert, 2004). In particular, $Y_{0,0}(\boldsymbol{u}) = \frac{1}{\sqrt{4\pi}}$, $\forall \boldsymbol{u} \in \mathcal{S}(0,1)$. Note that Eqs. (A.7) and (A.8) can be rewritten in the more compact form

$$\psi(\boldsymbol{u}, r) = \sum_{l\in\mathbb{N}} \boldsymbol{Y}_l\left(\boldsymbol{u}\right)^\top \boldsymbol{\psi}_l(r) \tag{A.9}$$

and

$$\boldsymbol{\psi}_l(r) = \int_{\boldsymbol{u}\in\mathcal{S}(0,1)} \boldsymbol{Y}_l(\boldsymbol{u})\, \psi(\boldsymbol{u}, r)\, dS(\boldsymbol{u}), \tag{A.10}$$

where $\forall l \in \mathbb{N}$, $\boldsymbol{Y}_l$ and $\boldsymbol{\psi}_l$ denote the $(2l+1)$-dimensional column vectors of coefficients $Y_{l,m}$ and $\psi_{l,m}$, respectively, for $m \in \{-l, \ldots, l\}$. In other respects, note that $\forall \boldsymbol{s} \in \partial V$,

$$\int_{\mathcal{S}(0,1)} \boldsymbol{Y}_{l_1}(\boldsymbol{u}) \boldsymbol{Y}_{l_2}(\boldsymbol{u} - 2(\boldsymbol{n}(\boldsymbol{s})^\top \boldsymbol{u})\boldsymbol{n}(\boldsymbol{s}))^\top dS(\boldsymbol{u}) = \boldsymbol{0}, \tag{A.11}$$

as soon as the vectors of real spherical harmonics $\boldsymbol{Y}_{l_1}$ and $\boldsymbol{Y}_{l_2}$ correspond to different eigenvalues of the Laplace operator on the unit sphere, i.e., as soon as $l_1 \neq l_2$. Indeed, we have $\forall l_1, l_2 \in \mathbb{N}$, $\forall m_1 \in \{-l_1, \ldots, l_1\}$, $\forall m_2 \in \{-l_2, \ldots, l_2\}$,

$$\begin{array}{rl} & -l_1(l_1+1) \int_{\mathcal{S}(0,1)} Y_{l_1,m_1}(\boldsymbol{u}) Y_{l_2,m_2}\left(\boldsymbol{u} - 2(\boldsymbol{n}(\boldsymbol{s})^\top \boldsymbol{u})\boldsymbol{n}(\boldsymbol{s})\right) dS(\boldsymbol{u}) \\ = & \int_{\mathcal{S}(0,1)} \Delta Y_{l_1,m_1}(\boldsymbol{u}) Y_{l_2,m_2}(\boldsymbol{u} - 2(\boldsymbol{n}(\boldsymbol{s})^\top \boldsymbol{u})\boldsymbol{n}(\boldsymbol{s})) dS(\boldsymbol{u}) \\ = & \int_{\mathcal{S}(0,1)} Y_{l_1,m_1}(\boldsymbol{u}) \Delta Y_{l_2,m_2}(\boldsymbol{u} - 2(\boldsymbol{n}(\boldsymbol{s})^\top \boldsymbol{u})\boldsymbol{n}(\boldsymbol{s})) dS(\boldsymbol{u}) \\ = & -l_2(l_2+1) \int_{\mathcal{S}(0,1)} Y_{l_1,m_1}(\boldsymbol{u}) Y_{l_2,m_2}\left(\boldsymbol{u} - 2(\boldsymbol{n}(\boldsymbol{s})^\top \boldsymbol{u})\boldsymbol{n}(\boldsymbol{s})\right) dS(\boldsymbol{u}), \end{array}$$

which implies, if $l_1 \neq l_2$,

$$\int_{\mathcal{S}(0,1)} Y_{l_1,m_1}(\boldsymbol{u}) Y_{l_2,m_2}(\boldsymbol{u} - 2(\boldsymbol{n}(\boldsymbol{s})^\top \boldsymbol{u})\boldsymbol{n}(\boldsymbol{s})) dS(\boldsymbol{u}) = 0,$$

which finally proves Eq. (A.11). Also, note that Eq. (A.11) implies that $\forall l_1 \neq l_2$,

$$\iint_{\mathcal{S}(0,1)} \boldsymbol{Y}_{l_1}(\boldsymbol{u}) A(\boldsymbol{u},\boldsymbol{v}) \boldsymbol{Y}_{l_2}(\boldsymbol{v})^\top dS(\boldsymbol{u}) dS(\boldsymbol{v}) = 0, \tag{A.12}$$

which shows that the linear operator A defined in Eq. (A.3) is block-diagonalizable in the basis of real spherical harmonics, as previously mentioned.

Therefore, if we substitute Eq. (A.9) into Eq. (A.1), if we then multiply the two members of the equality on the left by $\boldsymbol{Y}_l(\boldsymbol{u})$, and if we finally integrate over $\boldsymbol{u} \in \mathcal{S}(0,1)$ and substitute Eq. (A.11), we get

$$\frac{\partial \boldsymbol{\psi}_l(r)}{\partial r} = -\boldsymbol{A}_l \, \boldsymbol{\psi}_l(r), \tag{A.13}$$

where $\boldsymbol{A}_l$ is the $(2l+1) \times (2l+1)$ real symmetric positive semidefinite matrix defined in Eq. (16) (the positive semidefiniteness of matrix $\boldsymbol{A}_l$ follows from that of the linear operator A).

Therefore, in the same way as previously, the solution to the PDE in Eq. (A.13) converges to

$$\boldsymbol{\psi}_l(\infty) = \mathrm{Proj}_{\mathrm{Ker}(\boldsymbol{A}_l)} \, \boldsymbol{\psi}_l(0), \tag{A.14}$$

where $\mathrm{Proj}_{\mathrm{Ker}(\boldsymbol{A}_l)}$ denotes the $(2l+1) \times (2l+1)$ real symmetric positive semidefinite matrix of the orthogonal projection onto the subspace $\mathrm{Ker}(\boldsymbol{A}_l)$.

Finally, substituting Eqs. (A.14) and (A.10) for $r = 0$, into Eq. (A.9) for $r = +\infty$, yields

$$\psi(\boldsymbol{v}, \infty) = \int_{\boldsymbol{u} \in \mathcal{S}(0,1)} \psi(\boldsymbol{u}, 0) \, d\sigma(\boldsymbol{u}|\boldsymbol{v}), \tag{A.15}$$

where the directional measure σ is defined as in Eq. (17). Note that Eq. (15) can be retrieved from Eq. (A.15) if we replace $\psi(\boldsymbol{u}, 0)$ in the right member of Eq. (A.15) by $\psi(\boldsymbol{u})$, and $\psi(\boldsymbol{v}, \infty)$ in the left member of Eq. (A.15) by $\lim_{T \to +\infty} \frac{1}{T} \int_0^T \psi(\boldsymbol{v}(t)) \, dt$ with $\boldsymbol{v} = \boldsymbol{v}(0)$, as previously explained in Remark 6.

Let us now prove the assertion in Remark 4. We have proved in Remark 7 that the solution to the PDE in Eq. (A.2) converges to a function such that $\psi(\boldsymbol{v}, \infty) = \psi(\boldsymbol{v} - 2(\boldsymbol{n}(\boldsymbol{s})^\top \boldsymbol{v}) \, \boldsymbol{n}(\boldsymbol{s}), \infty)$ for almost every $\boldsymbol{s} \in \partial V$, which means that all functions in $\mathrm{Ker}(A)$ are invariant under the reflections through all 2D subspaces tangent to ∂V. In the same way, the same property holds for $\mathrm{Ker}(\boldsymbol{A}_L)$ at any degree $L \in \mathbb{N}$. Considering Eq. (18), this implies that

$$\sigma_L(\boldsymbol{u}, \boldsymbol{v}) = \sigma_L\left(\boldsymbol{u}, \boldsymbol{v} - 2(\boldsymbol{n}(\boldsymbol{s})^\top \boldsymbol{v}) \, \boldsymbol{n}(\boldsymbol{s})\right).$$

For $\boldsymbol{v} = \boldsymbol{n}(\boldsymbol{s})$, we thus get $\sigma_L(\boldsymbol{u}, \boldsymbol{n}(\boldsymbol{s})) = \sigma_L(\boldsymbol{u}, -\boldsymbol{n}(\boldsymbol{s}))$. In other respects, we have shown in Remark 1 that $\sigma_L(-\boldsymbol{u}, -\boldsymbol{v}) = \sigma_L(\boldsymbol{u}, \boldsymbol{v})$, therefore we can conclude that $\sigma_L(\boldsymbol{u}, \boldsymbol{n}(\boldsymbol{s})) = \sigma_L(-\boldsymbol{u}, \boldsymbol{n}(\boldsymbol{s}))$ for almost every $\boldsymbol{s} \in \partial V$. This finally proves Eq. (20).

Appendix B.

In this appendix, we derive the closed-form expression of the power spectrum $\widehat{\Gamma}_L$, which was given in Eq. (26). As in Badeau (2024, Sec. V A), we start by considering a local version $\widehat{\Lambda}_L(\mathcal{K}, \mathcal{V})$ of the spectral measure $\widehat{\Gamma}_B(\mathcal{K})$, first in a vicinity $\mathcal{V} \subset V$ of any interior point $\boldsymbol{s} \in V$ (Appendix Appendix B.1), then in a vicinity $\mathcal{V} \subset \overline{V}$ of any boundary point $\boldsymbol{s} \in \partial V$ (Appendix Appendix B.2), before introducing the consolidated expression of the spectral measure $\widehat{\Lambda}_L(\mathcal{K}, \mathcal{V})$ that holds in any region $\mathcal{V} \subseteq \overline{V}$ (Appendix Appendix B.3). The closed-form expression of $\widehat{\Gamma}_L$ is finally obtained for $\mathcal{V} = \overline{V}$.

Appendix B.1. Interior points

In a vicinity $\mathcal{V} \subset V$ of a point $\boldsymbol{s} \in V$, by using the mathematical developments in Badeau (2024, Sec. V A 1), we get $\widehat{\Lambda}(\boldsymbol{k}, \mathcal{V}) = \lambda^2 |\mathcal{V}|$. This equation can be integrated w.r.t. $\boldsymbol{k}$ on a Borel set $\mathcal{K} \subset \mathbb{R}^3$, in order to define a spectral measure $\widehat{\Lambda}_L(\mathcal{K}, \mathcal{V})$, rather than a spectral density function:

$$\widehat{\Lambda}_L(\mathcal{K}, \mathcal{V}) = \lambda^2 |\mathcal{K}||\mathcal{V}|. \tag{B.1}$$

In Eq. (B.1), the use of notation $\widehat{\Lambda}_L$ instead of $\widehat{\Lambda}$ is explained in Appendix Appendix B.2. Note that this spectral measure is innately isotropic (it corresponds to free field propagation), so that its expression is not affected by the successive reflections over the billiard's boundary.

Appendix B.2. Boundary points

As done in Balian and Bloch (1970, Sec. III-A), we now use the *plane approximation*: the boundary surface in the vicinity $\mathcal{V} \subset \overline{V}$ of a point $\boldsymbol{s} \in \partial V$, i.e., $\mathcal{V} \cap \partial V$, is approximated by $\mathcal{V} \cap T(\boldsymbol{s})$, where $T(\boldsymbol{s})$ denotes the plane tangent to ∂V at $\boldsymbol{s}$ (see Fig. 2 in Badeau (2024, Sec. IV C)). This approximation is justified at high frequency (see the second assumption in Sec. 4.2). By using the mathematical developments in Badeau (2024, Sec. V A 2), we get

$$\widehat{\Lambda}(\boldsymbol{k}, \mathcal{V}) = \lambda^2 \left(|\mathcal{V}| + \tfrac{S(\mathcal{V} \cap T(\boldsymbol{s}))}{4} \left(\tfrac{-1}{\imath \pi \boldsymbol{n}(\boldsymbol{s})^\top \boldsymbol{k}} + \delta(\boldsymbol{n}(\boldsymbol{s})^\top \boldsymbol{k}) \right) \right). \tag{B.2}$$

In Badeau (2024), we were interested in the particular case of mixing billiards that produce an isotropic wave field, so the next step consisted of integrating Eq. (B.2) for $\boldsymbol{k}$ on the sphere $\mathcal{S}(0, k)$ of radius $k \geq 0$, in order to get an expression of the power spectrum that is independent of the direction of vector $\boldsymbol{k}$, and depends only on its norm $k = \|\boldsymbol{k}\|_2$. The resulting expression of the power spectrum was thus independent of the outward normal $\boldsymbol{n}(\boldsymbol{s})$ of the boundary surface at $\boldsymbol{s}$. Here however, we consider the class of semi-mixing billiards defined by Eq. (14), which can generate an anisotropic wave field, so we need to proceed differently. Indeed, the successive reflections of vector $\boldsymbol{n}(\boldsymbol{s})$ (or, more precisely, of any ray trajectory of initial direction $\boldsymbol{v}(0) = \boldsymbol{n}(\boldsymbol{s})$) do not result in complete isotropy in the general case. On the contrary, we have shown in Sec. 3 that the dynamic reflection process results in a vector $\boldsymbol{u} \in \mathcal{S}(0, 1)$ that is distributed according to the directional measure $d\sigma(\boldsymbol{u}|\boldsymbol{n}(\boldsymbol{s}))$ over the unit sphere $\mathcal{S}(0, 1)$. Therefore the correct expression of the spectral measure is obtained by replacing $\boldsymbol{n}(\boldsymbol{s})$ in Eq. (B.2) by vector $\boldsymbol{u}$, and then by integrating the resulting expression w.r.t. the directional measure:

$$\widehat{\Lambda}_L(\boldsymbol{k},\mathcal{V}) = \lambda^2\Big(|\mathcal{V}| + \tfrac{S(\mathcal{V}\cap T(\boldsymbol{s}))}{4}\int_{\boldsymbol{u}\in\mathcal{S}(0,1)}\big(\tfrac{-1}{\imath\pi\boldsymbol{u}^\top\boldsymbol{k}} + \delta(\boldsymbol{u}^\top\boldsymbol{k})\big)\,\sigma_L(\boldsymbol{u},\boldsymbol{n}(\boldsymbol{s}))\,dS(\boldsymbol{u})\Big). \tag{B.3}$$

In Eq. (B.3), in the first place, the directional measure σ expressed in Eq. (17) has been replaced by its truncation to a finite degree L defined in Eq. (18). The notation $\widehat{\Lambda}_L$ instead of $\widehat{\Lambda}$ in Eqs. (B.1) and (B.3) reflects this dependence on the degree L. Then, for a reason that we explained in Remark 4, the integrand in Eq. (B.3) can be symmetrized w.r.t. $\boldsymbol{u}$ without changing the value of the integral:

$$\widehat{\Lambda}_L(\boldsymbol{k},\mathcal{V}) = \lambda^2\Big(|\mathcal{V}| + \tfrac{S(\mathcal{V}\cap T(\boldsymbol{s}))}{4}\int_{\boldsymbol{u}\in\mathcal{S}(0,1)}\delta(\boldsymbol{u}^\top\boldsymbol{k})\,\sigma_L(\boldsymbol{u},\boldsymbol{n}(\boldsymbol{s}))\,dS(\boldsymbol{u})\Big). \tag{B.4}$$

Finally, Eq. (B.4) can be integrated w.r.t. $\boldsymbol{k}$ on a Borel set $\mathcal{K}\subset\mathbb{R}^3$, in order to define a spectral measure $\widehat{\Lambda}_L(\mathcal{K},\mathcal{V})$ rather than a spectral density function:

$$\widehat{\Lambda}_L(\mathcal{K},\mathcal{V}) = \lambda^2\Big(|\mathcal{K}||\mathcal{V}| + \tfrac{S(\mathcal{V}\cap T(\boldsymbol{s}))}{4}\int_{\boldsymbol{k}\in\mathcal{K}}\int_{\boldsymbol{u}\in\mathcal{S}(0,1)}\delta\left(\boldsymbol{u}^\top\boldsymbol{k}\right)\,\sigma_L(\boldsymbol{u},\boldsymbol{n}(\boldsymbol{s}))\,dS(\boldsymbol{u})\,d\boldsymbol{k}\Big). \tag{B.5}$$

Appendix B.3. Consolidated spectral measure

In the same way as we did in Badeau (2024, Sec. V A 3), by integrating over all points $\boldsymbol{s}\in\overline{V}$, from Eqs. (B.1) and (B.5), we finally get the consolidated expression of the spectral measure $\widehat{\Lambda}_L$ on $\mathbb{R}^3\times\overline{V}$:

$$\widehat{\Lambda}_L(\mathcal{K},\mathcal{V}) = \lambda^2\Big(|\mathcal{K}||\mathcal{V}| + \tfrac{1}{4}\int_{\boldsymbol{k}\in\mathcal{K}}\int_{\boldsymbol{s}\in\mathcal{V}\cap\partial V}\int_{\boldsymbol{u}\in\mathcal{S}(0,1)}\delta\left(\boldsymbol{u}^\top\boldsymbol{k}\right)\,\sigma_L(\boldsymbol{u},\boldsymbol{n}(\boldsymbol{s}))\,dS(\boldsymbol{u})\,dS(\boldsymbol{s})\,d\boldsymbol{k}\Big), \tag{B.6}$$

where $dS(\boldsymbol{s})$ denotes the infinitesimal surface element that replaces $S(\mathcal{V}\cap T(\boldsymbol{s}))$ in Eq. (B.5).

Finally, the power spectrum $\widehat{\Gamma}_L(\boldsymbol{k})$ expressed in Eq. (26) was defined so that for any Borel set $\mathcal{K}\subset\mathbb{R}^3$,

$$\int_{\boldsymbol{k}\in\mathcal{K}}\widehat{\Gamma}_L(\boldsymbol{k})d\boldsymbol{k} = \widehat{\Lambda}_L(\mathcal{K},\overline{V}). \tag{B.7}$$

Note that $\widehat{\Gamma}_L(\boldsymbol{k})$ is an analytic function of $\boldsymbol{k}$ on $\mathbb{R}^3\backslash\{\boldsymbol{0}\}$. Indeed, Eq. (26) can be rewritten as:

$$\widehat{\Gamma}_L(\boldsymbol{k}) = \lambda\Big(1 + \tfrac{\lambda}{4\sqrt{\boldsymbol{k}^\top\boldsymbol{k}}}\int_{\boldsymbol{s}\in\partial V}\Big(\int_{\boldsymbol{u}\in\mathcal{S}(0,1)\cap\boldsymbol{k}^\perp}\sigma_L(\boldsymbol{u},\boldsymbol{n}(\boldsymbol{s}))dL(\boldsymbol{u})\Big)dS(\boldsymbol{s})\Big), \tag{B.8}$$

where $\boldsymbol{k}^\perp$ denotes the plane passing through the origin and orthogonal to vector $\boldsymbol{k}$, and $dL(\boldsymbol{u})$ denotes the length element on the unit circle $\mathcal{S}(0,1)\cap\boldsymbol{k}^\perp$. Moreover, it can be easily proved [e.g., by parametrizing $\mathcal{S}(0,1)\cap\boldsymbol{k}^\perp$ in the integral over $\boldsymbol{u}$ in Eq. (B.8)] that the analyticity of the function $\boldsymbol{u}\mapsto\sigma_L(\boldsymbol{u},\boldsymbol{v})$ (that has been shown in Remark 1) implies the analyticity of the function $\boldsymbol{k}\mapsto\int_{\boldsymbol{u}\in\mathcal{S}(0,1)\cap\boldsymbol{k}^\perp}\sigma_L(\boldsymbol{u},\boldsymbol{n}(\boldsymbol{s}))dL(\boldsymbol{u})$. Therefore the power spectrum $\widehat{\Gamma}_L(\boldsymbol{k})$ is an analytic function of $\boldsymbol{k}$ on $\mathbb{R}^3\backslash\{\boldsymbol{0}\}$. Consequently, the function $\boldsymbol{k}\mapsto\widehat{\Gamma}_L(\boldsymbol{k})$ in Eq. (B.8) can be analytically continued in the vicinity of $\mathbb{R}^3\backslash\{\boldsymbol{0}\}$ in $\mathbb{C}^3$, where $\sqrt{(.)}$ denotes the unique complex square root with a positive real part.

Appendix C.

In this appendix, we derive the closed-form expression of the causal source response p introduced in Eq. (3). Substituting Eq. (30) into Eq. (6) yields

$$\dot{g}(\boldsymbol{x},\boldsymbol{x}_0,t)=\mu_{\dot{g}}(t)-c^2\int_{\boldsymbol{k}\in\mathbb{R}^3}\left(\int_{f\in\mathbb{R}}\frac{2\imath\pi f\,e^{2\imath\pi\boldsymbol{k}^\top(\boldsymbol{x}-\boldsymbol{x}_0)}}{4\pi^2(f^2-c^2\|\boldsymbol{k}\|_2^2)}\,e^{2\imath\pi ft}df\right)d\widehat{B}_L(\boldsymbol{k}), \tag{C.1}$$

where Eq. (31) implies[8]

$$\mu_{\dot{g}}(t)=\int_{f\in\mathbb{R}}\mu_G(\tfrac{f}{c})\,2\imath\pi f\,e^{2\imath\pi ft}df=\tfrac{\lambda c^2}{2}\mathrm{sign}(t). \tag{C.2}$$

We note that the integrand in the integral over f in Eq. (C.1) has two real simple poles, one at $f=c\|\boldsymbol{k}\|_2$ and one at $f=-c\|\boldsymbol{k}\|_2$. By applying the residue theorem to Eq. (C.1), we get a simplified expression of $\dot{g}(\boldsymbol{x},\boldsymbol{x}_0,t)$[9]:

$$\dot{g}(\boldsymbol{x},\boldsymbol{x}_0,t)=\mu_{\dot{g}}(t)+\tfrac{c^2}{2}\mathrm{sign}(t)\int_{\boldsymbol{k}\in\mathbb{R}^3}\cos(2\pi c\|\boldsymbol{k}\|_2t)e^{2\imath\pi\boldsymbol{k}^\top(\boldsymbol{x}-\boldsymbol{x}_0)}d\widehat{B}_L(\boldsymbol{k}). \tag{C.3}$$

Finally, by substituting Eq. (C.3) into Eq. (7), we get Eqs. (32) and (33).

Appendix D.

In this appendix, we derive the expression of the power distribution in Eq. (36). When $\boldsymbol{x}_1=\boldsymbol{x}_2=\boldsymbol{x}$, substituting Eq. (26) into Eq. (35) yields

$$\begin{aligned}
&W_q(\boldsymbol{x},\boldsymbol{x},\boldsymbol{x}_0,f,t)\\
=\;&\tfrac{c^3}{4}\int_{\boldsymbol{k}\in\mathcal{S}(0,\frac{|f|}{c})}\widehat{\Gamma}_L(\boldsymbol{k})dS(\boldsymbol{k})\\
=\;&\tfrac{\lambda c^3}{4}\int_{\boldsymbol{k}\in\mathcal{S}(0,\frac{|f|}{c})}\left(1+\tfrac{\lambda}{4}\int_{\boldsymbol{s}\in\partial V}\left(\int_{\boldsymbol{u}\in\mathcal{S}(0,1)}\delta\left(\boldsymbol{u}^\top\boldsymbol{k}\right)\,\sigma_L(\boldsymbol{u},\boldsymbol{n}(\boldsymbol{s}))\,dS(\boldsymbol{u})\right)dS(\boldsymbol{s})\right)dS(\boldsymbol{k})\\
=\;&\tfrac{\lambda c^3}{4}\left(4\pi\tfrac{f^2}{c^2}+\tfrac{\lambda}{4}\int_{\boldsymbol{s}\in\partial V}\left(\int_{\boldsymbol{u}\in\mathcal{S}(0,1)}\left(\int_{\boldsymbol{k}\in\mathcal{S}(0,\frac{|f|}{c})}\delta\left(\boldsymbol{u}^\top\boldsymbol{k}\right)dS(\boldsymbol{k})\right)\sigma_L(\boldsymbol{u},\boldsymbol{n}(\boldsymbol{s}))\,dS(\boldsymbol{u})\right)dS(\boldsymbol{s})\right)\\
=\;&\pi\lambda cf^2+\tfrac{\lambda^2c^3}{16}\int_{\boldsymbol{s}\in\partial V}\left(\int_{\boldsymbol{u}\in\mathcal{S}(0,1)}2\pi\tfrac{|f|}{c}\,\sigma_L(\boldsymbol{u},\boldsymbol{n}(\boldsymbol{s}))\,dS(\boldsymbol{u})\right)dS(\boldsymbol{s})\\
=\;&\pi\lambda cf^2+\tfrac{\pi\lambda^2c^2|f|}{8}\int_{\boldsymbol{s}\in\partial V}dS(\boldsymbol{s}),
\end{aligned}$$

since $\int_{\boldsymbol{u}\in\mathcal{S}(0,1)}\sigma_L\left(\boldsymbol{u},\boldsymbol{n}(\boldsymbol{s})\right)\,dS(\boldsymbol{u})=1$, as proved in Remark 1. We thus finally retrieve the closed-form expression of the power distribution in Eq. (36).

[8] The last member of Eq. (C.2) is obtained by applying the residue theorem to the middle member. Note that two different integration contours must be considered depending on the sign of t, and that the simple pole at $f=0$ belongs to both contours, so the corresponding residue is divided by two.

[9] Again, note that two different integration contours must be considered depending on the sign of t, and that the two simple poles at $f=c\|\boldsymbol{k}\|_2$ and $f=-c\|\boldsymbol{k}\|_2$ belong to both contours, so the corresponding residues are divided by two.

References

Alary, B. (**2021**). "Analysis and synthesis of directional reverberation," Ph.D. thesis, Aalto University, Aalto, Finland.

Alary, B., Politis, A., and Bilbao, S. (**2024**). "Designing directional reverberators for spatial sound reproduction," in *Proceedings of the AES 5th International Conference on Audio for Virtual and Augmented Reality*, Redmond, WA, pp. 1–4.

Alary, B., Politis, A., Schlecht, S., and Välimäki, V. (**2019**). "Directional feedback delay network," Journal of the Audio Engineering Society **67**(10), 752–762.

Arana-Herrera, F., Chaika, J., and Forni, G. (**2025**). "Weak mixing in rational billiards," Annals of Mathematics In press (accepted 2025-08-13).

Arendt, W., Nittka, R., Peter, W., and Steiner, F. (**2009**). "Weyl's law: Spectral properties of the Laplacian in mathematics and physics," in *Mathematical Analysis of Evolution, Information, and Complexity* (Wiley-VCH, Weinheim, Germany), Chap. 1, pp. 1–71.

Arnold, V. I., and Avez, A. (**1989**). *Ergodic problems of classical mechanics* (Addison-Wesley, Boston, MA).

Badeau, R. (**2024**). "Statistical wave field theory," J. Acoust. Soc. Am. **156**(1), 573–599.

Badeau, R. (**2025**a). "On the spectral decomposition of the complex Robin Laplacian," J. Acoust. Soc. Am. **158**(1), 838–848.

Badeau, R. (**2025**b). "Statistical wave field theory: Curvature term," J. Acoust. Soc. Am. **157**(3), 1650–1664.

Badeau, R. (**2025**c). "Statistical wave field theory: Special polyhedra," J. Acoust. Soc. Am. **157**(3), 2263–2278.

Balian, R., and Bloch, C. (**1970**). "Distribution of eigenfrequencies for the wave equation in a finite domain: I. Three-dimensional problem with smooth boundary surface," Ann. Phys. **60**(2), 401–447.

Balian, R., and Bloch, C. (**1972**). "Distribution of eigenfrequencies for the wave equation in a finite domain: III. Eigenfrequency density oscillations," Ann. Phys. **69**(1), 76–160.

Berry, M. V. (**1977**). "Regular and irregular semiclassical wavefunctions," Journal of Physics A: Mathematical and General **10**(12), 2083–2091.

Berzborn, M., and Vorländer, M. (**2021**). "Directional sound field decay analysis in performance spaces," Building Acoustics **28**(3), 249–263.

Bilbao, S., and Alary, B. (**2024**). "Directional reverberation time and the image source method for rectangular parallelepipedal rooms," J. Acoust. Soc. Am. **155**(2), 1343–1352.

Brack, M., and Bhaduri, R. (**1997**). *Semiclassical Physics* (Addison-Wesley, Boston, MA).

Cohen, L. (**1989**). "Time-frequency distributions–A review," Proc. IEEE **77**(7), 941–981.

Cook, R. K., Waterhouse, R., Berendt, R., Edelman, S., and Thompson, M. (**1955**). "Measurement of correlation coefficients in reverberant sound fields," J. Acoust. Soc. Am. **27**(6), 1072–1077.

Courant, R., and Hilbert, D. (**2004**). "Special functions defined by eigenvalue problems," in *Methods of Mathematical Physics* (Wiley-VCH, Weinheim, Germany), Chap. 7, pp. 466–549.

Daley, D. J., and Vere-Jones, D. (**2003**). Probability and its Applications *An introduction to the theory of point processes. Volume I: Elementary Theory and Methods*, 2nd ed. (Springer-Verlag, New York).

Drechsler, S. (**2012**). "The anisotropic reverberation model (ARM) - a simplified method to calculate the sound energy decay and derived properties," in *Proceedings of the 41st International Congress and Exposition on Noise Control Engineering (INTER-NOISE)*, pp. 1–11.

Drechsler, S., and Stephenson, U. M. (**2012**). "A calculation model for anisotropic reverberation with specular and diffuse reflections," in *Proceedings of the DAGA 2012 annual conference on acoustics*, pp. 605–606.

Eyring, C. F. (**1930**). "Reverberation time in 'dead' rooms," J. Acoust. Soc. Am. **1**(2A), 217–241.

Götz, G., Schlecht, S. J., and Pulkki, V. (**2023**). "Common-slope modeling of late reverberation," IEEE/ACM Transactions on Audio, Speech, and Language Processing **31**, 3945–3957.

Grebenkov, D. S., and Nguyen, B.-T. (**2013**). "Geometrical structure of Laplacian eigenfunctions," SIAM Review **55**(4), 601–667.

Gutzwiller, M. C. (**1971**). "Periodic orbits and classical quantization conditions," Journal of Mathematical Physics **12**(3), 343–358.

Hassell, A., and Hillairet, L. (**2010**). "Ergodic billiards that are not quantum unique ergodic," Annals of Mathematics **171**(1), 605–618.

Joyce, W. B. (**1978**). "Exact effect of surface roughness on the reverberation time of a uniformly absorbing spherical enclosure," J. Acoust. Soc. Am. **64**(5), 1429–1436.

Kanev, N. G. (**2012**). "Sound decay in a rectangular room with impedance walls," Acoustical Physics **58**(5), 603–609.

Kerckhoff, S., Masur, H., and Smillie, J. (**1986**). "Ergodicity of billiard flows and quadratic differentials," Annals of Mathematics **124**(2), 293–311.

Kuttruff, H. (**2014**). *Room Acoustics, 5th ed.* (CRC Press, Boca Raton, FL), pp. 1–374.

Lu, Z., Graf, A. M., Heller, E. J., Keski-Rahkonen, J., and Dag, C. B. (**2025**). "Antiscarring from eigenstate stacking in a chaotic spinor condensate," Phys. Rev. A **112**, 043307.

Marklof, J., and Rudnick, Z. (**2012**). "Almost all eigenfunctions of a rational polygon are uniformly distributed," J. Spectr. Theory **2**(1), 107–113.

Meyer-Kahlen, N., and Schlecht, S. J. (**2024**). "Directional distribution of the pseudo intensity vector in anisotropic late reverberation," J. Acoust. Soc. Am. **155**(2), 1515–1526.

Morse, P. M., and Ingard, K. U. (**1968**). *Theoretical acoustics* (McGraw-Hill, New York).

Nolan, M., Fernandez-Grande, E., Brunskog, J., and Jeong, C.-H. (**2018**). "A wavenumber approach to quantifying the isotropy of the sound field in reverberant spaces," J. Acoust. Soc. Am. **143**(4), 2514–2526.

Polack, J.-D. (**1992**). "Modifying chambers to play billiards: the foundations of reverberation theory," Acta Acust. united Acust. **76**(6), 257–272.

Polack, J.-D. (**2025**). "Revisiting reverberation," Acta Acustica **9**(30), 1–19.

Poletti, M. A. (**2005**). "Three-dimensional surround sound systems based on spherical harmonics," Journal of the Audio Engineering Society **53**(11), 1004–1025.

Sieber, M., Primack, H., Smilansky, U., Ussishkin, I., and Schanz, H. (**1995**). "Semiclassical quantization of billiards with mixed boundary conditions," Journal of Physics A: Mathematical and General **28**(17), 5041–5078.

Tabachnikov, S. (**1995**). Panoramas et synthèses (*Panoramas and overviews*) *Billiards* (Société mathématique de France, Paris, France).

Weyl, H. (**1911**). "Ueber die asymptotische verteilung der eigenwerte (*On the asymptotic distribution of eigenvalues*)," Nachr. von der Gesellschaft der Wissenschaften zu Göttingen, Mathematisch-Physikalische Klasse **1911**, 110–117.

Xu, Q., Shen, X., Peng, P., Loh, T. H., and Huang, Y. (**2022**). "Alternative definitions of the field anisotropy in a reverberation chamber," in *Proceedings of the 2022 3rd URSI Atlantic and Asia Pacific Radio Science Meeting (AT-AP-RASC)*, pp. 1–4.

Zelditch, S. (**2006**). "Quantum ergodicity and mixing of eigenfunctions," in *Encyclopedia of mathematical physics*, edited by J.-P. Françoise, G. L. Naber, and T. S. Tsun, **1** (Academic Press/Elsevier Science, Oxford, UK).

Zelditch, S., and Zworski, M. (**1996**). "Ergodicity of eigenfunctions for ergodic billiards," Communications in Mathematical Physics **175**(3), 673–682.